Some studies on the load carrying capacity of shallow foundation resting over geogrid-reinforced sand under eccentric load

A Thesis Submitted in Partial Fulfillment of the Requirements for the Degree of

Master of Technology
In
Civil Engineering

ROMA SAHU

DEPARTMENT OF CIVIL ENGINEERING

NATIONAL INSTITUTE OF TECHNOLOGY, ROURKELA

2013

Some studies on the load carrying capacity of shallow foundation resting over geogrid-reinforced sand under eccentric load

A Thesis Submitted in Partial Fulfillment of the Requirements for the Degree of

Master of Technology
in
Civil Engineering

Under the guidance and supervision of

Prof C.R.Patra

Submitted By:

ROMA SAHU

(ROLL NO. 211CE1232)

DEPARTMENT OF CIVIL ENGINEERING

NATIONAL INSTITUTE OF TECHNOLOGY, ROURKELA

2013

National Institute of Technology
Rourkela

CERTIFICATE

This is to certify that the thesis entitled "***Some studies on the load carrying capacity of shallow foundation resting over geogrid-reinforced sand under eccentric load***" being submitted by Roma Sahu in partial fulfillment of the requirements for the award of **Master of Technology** Degree in **Civil Engineering**with specialization in **GEOTECHNICAL ENGINEERING** at National Institute of Technology Rourkela, is an authentic work carried out by her under my guidance and supervision.

To the best of my knowledge, the matter embodied in this report has not been submitted to any other university/institute for the award of any degree or diploma.

Dr. ChittaranjanPatra
Professor
Department of Civil Engineering
NIT Rourkela

Place: Rourkela
Date: 31.05.2013

ACKNOWLEDGEMENTS

First of all, I would like to express my sincere gratitude to my supervisor **Prof**. **Chittaranjan Patra**, for his guidance and constant encouragement and support during the course of my work in the last one year. I truly appreciate and value his esteemed guidance and encouragement from the beginning to the end of the thesis.

I would like to thank **Prof. N Roy**, **Head of the Dept. of Civil Engineering,** National Institute of technology, Rourkela, who have enlightened me during my project.

I am also thankful to **Prof. S.K. Das**, **Prof. S.P. Singh** and all professors of Civil Engineering Department.

A special words of thanks to **Mr. Rabi Narayan Behera**, Ph.D. scholar of Civil Engineering Department, for his suggestions, comments and entire support throughout the project work.

I am also thankful to staff members of Geotechnical Engineering Laboratory especially Mr. Rajesh, Mr. Chamuru suniani, Mr. Harihar Garnayak for their assistance &co-operation during the exhaustive experiments in the laboratory. I express to my special thanks to my dear friends Sonia, Swagatika, Jajati , Sumant, Manaswini, Laxmi. Saini, Mona, Tulika, Usha for their continuous support, suggestions and love.

Friendly environment and cooperative company I had from my classmates and affection received from my seniors and juniors will always remind me of my days as a student at NIT Rourkela. I wish to thank all my friends and well-wishers who made my stay at NIT Rourkela, memorable and pleasant.

Finally, I would like to thank my parents and family members for their unwavering support and invariable source of motivation.

Roma Sahu

ABSTRACT

Several works have been done relating to the estimate of the ultimate bearing capacities of shallow foundations, supported by geogrid reinforced sand. Few experimental studies have been made on the evaluation of bearing capacity of shallow foundations on geogrid-reinforced sand under eccentric load. These studies relate to strip and a square foundation is yet to be done.

The purpose of this thesis is to conduct few model tests in the laboratory by using square surface foundation over the reinforced sand bed. The model footing used for the model tests in the laboratory is of size 10cm x 10cm. The average relative density maintained during all the tests is 69%. The reinforcing material used in the experiment is SS 20 in 2, 3 and 4 number of layers. The load eccentricity is varied from 0 to 0.15*B* with an increment of 0.05*B*. The vertical distance of first geogrid layer from base, distance between the consecutive geogrid layers, and width of the geogrid has been kept constant. For each set up load intensity and corresponding settlements are observed which are plotted to get load-settlement curves for each set up. The load-settlement curve for each test is plotted to determine the ultimate bearing capacity. Parametric studies have been made to evaluate the influence of load eccentricity on bearing capacity of the foundation. The ultimate bearing capacity of eccentrically loaded square footings can be computed by knowing the ultimate bearing capacity of square footing under central load and a reduction factor (R_{kR}) for reinforced condition. The reduction factor is developed based on the results of laboratory model tests on geogrid reinforced soil.

The existing data base of Patra et al. (2006) is used for predicting bearing capacity of strip footings over geogrid reinforced soil under eccentric load by using Artificial Neural Network (ANN).

TABLE OF CONTENTS

Title **Page No.**

LIST OF TABLES

LIST OF FIGURES

Title **Page No**

LIST OF NOTATIONS

B	Width of foundation
L	Length of foundation
t	Thickness of foundation
e	Load eccentricity
u	Location of the top layer of reinforcement from the bottom the foundation
d	Depth of reinforcement layer
N	Number of reinforcement layer
h	Vertical distance between two consecutive layers
b	width of reinforcement layer
l	length of reinforcement layer
d_f	Total depth from the bottom of foundation to depth of reinforcement layer.
α	Load inclination with the vertical
Q_u	Ultimate load per unit length of the foundation
γ	Unit weight of sand
γ_d	Dry unit weight of sand
$\gamma_{d(max)}$	Maximum dry unit weight of sand
$\gamma_{d(min)}$	Minimum dry unit weight of sand
ϕ	Friction angle of sand
ϕ'	Effective friction angle of sand
q_u	Ultimate bearing capacity
N_c, N_q, N_γ	Bearing capacity factors
s_c, s_q, s_γ	Shape factors

s	Settlement
B'	Effective width of foundation
A'	Effective area of foundation
C_u	Coefficient of uniformity
C_c	Coefficient of curvature
G	Specific gravity
D_{10}	Effective particle size
D_{50}	Mean particle size
D_r	Relative Density
r	Correlation coefficient
R^2	Coefficient of efficiency
er	Residual

CHAPTER 1

INTRODUCTION

Chapter 1 INTRODUCTION

Foundation is an integral part of a structure whether it may be a building, bridge and dam etc. The function of the foundation is to receive the load from the superstructure and transmit it to the underlying soil or rock.

Soil is used as a construction material for various civil engineering structures. Structure on a ground with adequate bearing capacity is one of the basic requirements for the stability of a structure. Most of the studies for bearing capacity calculation are based on the foundation under vertical and central load. However in some cases due to bending moments and horizontal thrusts transferred from the superstructure, structures like retaining walls, abutments, waterfront structures, industrial machines and portal framed buildings are often subjected to eccentric load. This may be due to (a) moments with or without axial forces (b) the oblique loading and (c) their location near the property line etc. When the load is transferred at the base of the footing, movement of the soil particles in the horizontal and vertical direction occurs. For the footings under eccentric loading, the two edges settle by different amounts, causing the footing tilt. The amount of tilt and the pressure at the base depend upon the value of eccentricity width ratio (e/B). When this ratio is more than 1/6, the contact pressure will be tensile at the edge away from the load. However, since the soil is poor in tension, such situation cannot develop; hence, the footing loses contact with the soil and tilting of the footing occurs. Due to eccentric loading, the footing tilts and the pressure below the footing does not remain uniform. The tilt of footing increases with an increase in the eccentricity and the bearing capacity reduces. Many times reinforcing materials like geogrid, geotextile, geonet etc. are inserted into the granular materials to improve the bearing capacity of poor sub-soil.

Over the last two decades the use of geogrids for soil reinforcement has increased greatly because geogrids are dimensionally stable and combine feature such as high tensile modulus

(low strain at high load), open geogrid structure, positive shear connection characteristics, light weight, and long service life. Geogrids are made of high-modulus polymer materials, such as polypropylene and polyethylene, and are prepared by tensile drawing. Nelton Ltd. of the United Kingdom was the first producer of geogrids in 1982. The major function of geogrid is soil reinforcement interaction. There are two types of geogrid i.e. uniaxial and biaxial depending on the nature of manufacturing.

A number of laboratory test results and a few field test results have been published that relate to the ultimate and allowable bearing capacity of shallow foundations supported by multi-layered geogrid reinforced sand and clay. The techniques of ground improvement by providing reinforcement were also in practice in olden days. Babylonians built ziggurats more than three thousand years ago using the principles of soil reinforcement. A part of the Great Wall of China is also an example of reinforced soil. Basic principles underlying reinforced soil was not completely investigated till Henry Vidal of France (1966) who introduced the reinforcing mechanism.

CHAPTER 2

LITERATURE REVIEW

2.1 INTRODUCTION

Foundation is a lowest part of structure which transmits the load of superstructure to underlying soil. Foundation is of two types: shallow and deep foundation. In case of shallow foundation soil layer for supporting a structure at a relatively shallow depth but in case of deep foundation the upper layer of soil is not suitable to carry a structure. The weight of the structure is transferred to stable layer at a greater depth (piles, piers, caissons). The loads of the structures are transmitted to the underlying soils through the base of the foundations. The soil, which is a compressible material, is compressed due to the stresses transmitted to it. Apart from vertical axial loads, the foundations of portal-framed buildings are often subjected to eccentric loads caused by wind and earthquake forces. Sometimes the corner column of these portal-framed buildings is located very close to the property line, and hence subjected to the eccentric loading. Foundations of earth retaining structures, abutments, and similar structures may be subjected to eccentric loading caused by the moments in addition to the axial forces. Eccentric load due to (i) moments with or without axial forces (ii) the oblique loading (iii) their location near the property line. The two edges settle by different amounts, and the footing will be tilt. The amount of tilt and the pressure at the base depend upon the value of the eccentricity width ratio. When this eccentricity width ratio is more than 1/6, the contact pressure will be tensile. However, since the soil is not a tension medium, thus, this type of situation cannot develop; hence, the footing loses contact with the soil and causing the footing tilt. Due to eccentric loading, the footing tilts and the pressure below the footing does not remain uniform. The footing tilt increases with an increase in the eccentricity and the bearing capacity reduces. Mechanically stabilized earth (MSE) technology is now well established in the heavy construction industries as a reliable and useful method in the construction of structures such as retaining walls, embankment over soft soil, steep slopes and

various other structures. MSE is a composite material consisting of compacted soil fill strengthened by the inclusion of tensile elements such as geogrid, geotextiles, metal rods and/or strips. Geogrid are relatively stiff material compared to geotextiles. They develop reinforcing strength at low strain level such as 2%. Therefore, it is intended to study the mechanism of shallow square foundations subjected to eccentric load underlying the geogrid reinforced soil mass.

2.1.1 Bearing capacity of foundation on homogeneous soil under central loading condition

The stability of a structure depends upon the stability of the supporting soil. For that the foundation must be stable against shear failure of the supporting soil and must not settle beyond a tolerable limit to avoid damage to the structure. For a given foundation to perform its optimum capacity, one must be ensured that it does not exceed its ultimate bearing capacity. The ultimate bearing capacity (q_u) is defined as the pressure at which shear failure occurs in the supporting soil immediately below and adjacent to the foundation. Some important landmark theories on bearing capacity developed by the investigators in the past based on experimental and analytical studies are discussed in this section.

Terzaghi (1948) proposed a theory to determine the ultimate bearing capacity of a shallow, rough, rigid continuous (strip) foundation supported by a homogeneous soil layer. The equation can be expressed as

$$q_u = cN_c + qN_q + 1/2\gamma BN_\gamma \text{ (Continuous foundation)} \quad (2.1)$$

$$q_u = 1.3cN_c + qN_q + 0.4\gamma BN_\gamma \text{ (Square foundation)} \quad (2.2)$$

$$q_u = 1.3cN_c + qN_q + 0.3\gamma BN_\gamma \text{ (Circular foundation)} \quad (2.3)$$

For granular soil the equation 2.1 is reduced to the form as expressed by:

$$q_u = qN_q + 1/2\gamma BN_\gamma \quad (2.4)$$

Meyerhof (1951) suggested a generalized method to estimate the ultimate bearing capacity for centrally vertically loaded foundation as

$$q_u = cN_c\lambda_{cs}\lambda_{cd} + qN_q\lambda_{qs}\lambda_{qd} + \frac{1}{2}\gamma BN_\gamma\lambda_{\gamma s}\lambda_{\gamma d} \quad (2.5)$$

For granular soil the above equation (2.5) can be reduced to the form as

$$q_u = qN_q\lambda_{qs}\lambda_{qd} + \frac{1}{2}\gamma BN_\gamma \quad (2.6)$$

q_u = ultimate bearing capacity for a soil, $q = \gamma D_f$ = surcharge, D_f = depth of embedment, B = width of the foundation. c = unit cohesion. $\lambda_{cs,}\lambda_{qs,}\lambda_{\gamma s}$ = shape factors $\lambda_{cd,}\lambda_{qd,}\lambda_{\gamma d}$ = depth factors, $N_{c,}N_{q,}N_\gamma$ =bearing capacity factors.

In the past many investigators have proposed bearing capacity factors as well as shape and depth factors for estimating the bearing capacity of footings in above conditions. These factors are summarized in table 2.1

Table 2.1: Summary of bearing capacity factors

Bearing Capacity Factors	Equation	Investigator
N_c	$N_c = (N_q - 1)\cot\phi$	Prandtl (1921), Reisnner (1924), Terzaghi (1943), Meyerhof (1963)
N_c	$N_c = \frac{228 + 4.3\phi}{40 - \phi}$	Krizek (1965)
N_q	$N_q = \tan^2(45 + \frac{\phi}{2})e^{\Pi\tan\phi}$	Prandtl (1921), Reisnner (1924), Terzaghi (1943), Meyerhof (1963)
N_q	$N_q = \frac{40 + 5\phi}{40 - \phi}$	Krizek (1965)
N_q	$N_q = \frac{e^{2\left(\frac{3\Pi}{4} - \frac{\phi}{2}\right)}\tan\phi}{2\cos\left(45 + \frac{\phi}{2}\right)^2}$	Terzaghi (1943)
N_γ	$N_\gamma = 1.8(N_q - 1)\cot\phi(\tan\phi)^2$	Terzaghi (1943)
N_γ	$N_\gamma = 1.5(N_q - 1)\tan\phi$	Lundgren and Mortensen (1953) and Hansen (1970)
N_γ	$N_\gamma = 1.8(N_q - 1)\tan\phi$	Biarez et al (1961)
N_γ	$N_\gamma = 2(N_q + 1)\tan\phi$	Vesic (1973)
N_γ	$N_\gamma = 1.5N_c\tan\phi^2$	Hansen (1970)
N_γ	$N_\gamma = (N_q - 1)\tan(1.4\phi)$	Meyerhof (1963)

Summary of shape factors

Factors	Equation	Investigator
Shape	For ϕ=0, $S_c = 1 + 0.2(\frac{B}{L})$ $S_q = S_\gamma = 1$ For ϕ> 10, $S_c = 1 + 0.2\left(\frac{B}{L}\right)\tan\left(45 + \frac{\phi}{2}\right)^2$	Meyerhof (1963)

	$S_q = S_\gamma = 1 + 0.1\left(\frac{B}{L}\right)\tan\left(45 + \frac{\phi}{2}\right)^2$	
	$S_c = 1 + \left(\frac{N_q}{N_c}\right)\left(\frac{B}{L}\right)$ [Use N_c and N_q given by Meyerhof (1963)] $S_q = 1 + \left(\frac{B}{L}\right)\tan\phi$ $S_\gamma = 1 - 0.4\left(\frac{B}{L}\right)$	DeBeer (1970),Vesic (1975)
	$S_c = 1 + \left(1.8(\tan\phi)^2 + 0.1\right)\left(\frac{B}{L}\right)^{0.5}$ $S_q = 1 + 1.9(\tan\phi)^2\left(\frac{B}{L}\right)^{0.5}$ $S_\gamma = \left(1 + 0.6(\tan\phi)^2 - 0.25\right)\left(\frac{B}{L}\right)$ $S_\gamma = 1 + \left(1.3(\tan\phi)^2 - 0.5\right)\left(\frac{L}{B}\right)^{1.5} e^{-\left(\frac{L}{B}\right)}$	Michalowski (1997)

2.1.2 Bearing capacity of foundation on homogeneous soil under eccentric loading condition

Meyerhof (1953) proposed a semi-empirical procedure to estimate the ultimate bearing capacity of shallow foundation subjected to eccentric loading which is generally referred to as the "equivalent area method". The ultimate bearing capacity $q_{u(e)}$ can be expressed as

$$q_{u(e)} = cN_c\lambda_{cd} + qN_q\lambda_{qd} + \frac{1}{2}\gamma B' N_\lambda \lambda_{\gamma d} \tag{2.7}$$

For granular soil the Equation 2.10 is reduced to the form as expressed by

$$q_{u(e)} = qN_q\lambda_{qd} + \frac{1}{2}\gamma B' N_\lambda \lambda_{\gamma d} \tag{2.8}$$

Where, $q_{u(e)}$ = ultimate bearing capacity with load eccentricity e, $q = \gamma D_f$, γ is the unit weight of soil, D_f =depth of foundation, B is the width of foundation, $B' = B - 2e$, e is the load eccentricity, $N_{q,} N_{\gamma}$ are the bearing capacity factors, $F_{qd,} F_{\gamma d}$ are the depth factor.

$Q = qA'$

Where A' = effective area =B'×1 (for strip footing)

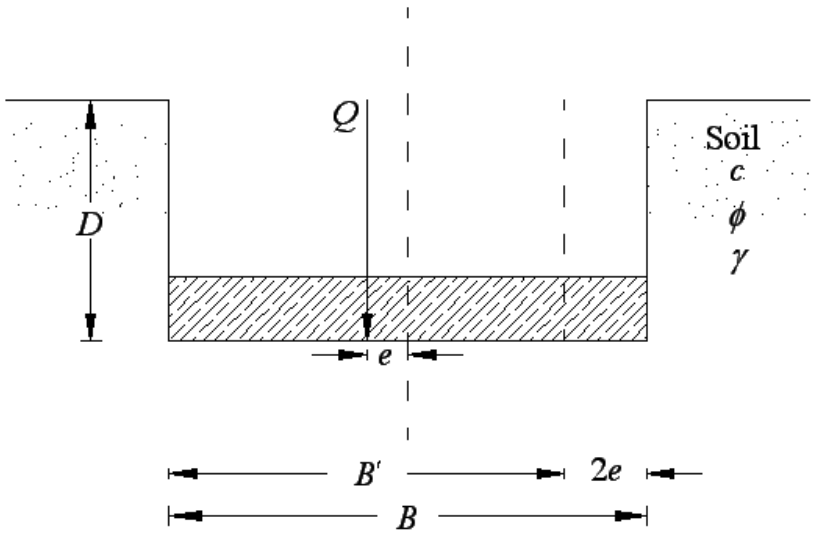

Figure 2.1: Eccentrically loaded footing (Meyerhof, 1953)

Purkayastha and char (1977) carried out stability analysis of eccentrically loaded strip foundation on sand using the method of slices proposed by Janbu (1957). Based on this study, they proposed that

$$\frac{q_{u(e)}}{q_{u(e=0)}} = 1 - R_K \tag{2.9}$$

$$R_K = 1 - \frac{q_{u(eccentric)}}{q_{u(centric)}} \tag{2.10}$$

Where, R_k = Reduction factor, $q_{u(eccentric)}$ = ultimate bearing capacity of eccentrically loaded continuous foundations, $q_{u(centric)}$ = ultimate bearing capacity of centrally loaded continuous foundations.

Where,

R_K = Reduction factor $= a\left(\frac{e}{B}\right)^K$ (2.11)

where, a and k are functions of the embedment ratio D_f / B

The values of a and k are presented in table 2.2 for different D_f / B

Table 2.2: Values of a and k

D_f/B	a	k
0.00	1.862	0.73
0.25	1.811	0.785
0.50	1.754	0.80
1.00	1.820	0.888

Combining equations 2.10 & 2.11

$$q_{u(eccentric)} = q_{u(centric)}(1 - R_K) = q_{u(centric))}\left[1 - a\left(\frac{e}{B}\right)\right]^K \quad (2.12)$$

$$q_{u(centric)} = qN_q\lambda_{qd} + \frac{1}{2}\gamma BN_\gamma\lambda_{\gamma d} \qquad \text{(c = 0)} \quad (2.13)$$

From the analysis they concluded that the width of footing and friction angle has no influence on reduction factor.

Prakash and saran (1971) presented a comprehensive mathematical formulation to estimate the ultimate bearing capacity for a rough foundation under eccentric loading. According to this theory for a strip foundation on sand

$$q_u = \frac{Q_u}{B \times 1} = cN_{C(e)} + \gamma D_f N_{q(e)} + \frac{1}{2}\gamma B N_{\gamma(e)} \qquad (2.14)$$

Where, $N_{c(e),} N_{q(e),N_{\gamma(e)}}$ are the bearing capacity factors for an eccentrically loaded continuous foundation. The bearing capacity factors are functions of *e/B* and ϕ. The bearing capacity factors are presented in the form of figure for different *e/B* and ϕ.

Michalowski and You (1998) presented the bearing capacity of eccentrically loaded footing using the kinematic approach of limit analysis. Meyerhof suggested that for eccentricity of loading, footing width is reduced by twice-the-eccentricity to its effective size and sometimes this hypothesis has been criticized as over conservative. The effective width rule significantly underestimates the bearing capacity for clays (ϕ = 0) only when the footing is bonded with the soil and the eccentricity is relatively large (*e/B* >0.25). For cohesive-frictional soils this underestimation decreases with an increase in the internal friction angle. The rule of effective width gives very reasonable estimates of the bearing capacity of eccentrically loaded footings on cohesive or cohesive-frictional soils when the soil-footing interface is not bonded, and for any type of interface when the eccentricity is small (*e/B* < 0.1). It also overestimates the bearing capacity for purely frictional soils when the surcharge load is relatively small. For cohesionless however, the effective width rule may overestimate the best upper bound and this overestimation increases with an increase in eccentricity.

Mahiyar and Patel (2000) carried out finite-element analysis of an angle shaped footing under eccentric loading. One side vertical projection of footing confines the soil and prevents its lateral

movement. It was concluded that footing subjected to uniaxial eccentric loads can be designed for no or negligible tilt.

2.1.3 Bearing capacity of Foundations supported over soil geogrid-reinforced soil

Some works done by the past investigators on the bearing capacity of shallow foundation on geogrid reinforced soil are briefly described in this section.

During the last twenty years, a number of laboratory model test results and a few field test results have been published that related to the ultimate and allowable bearing capacity of shallow foundations supported by multi-layered geogrid reinforced sand and clay. Some of the investigators have evaluated the beneficial effect of using geogrid as a soil reinforcement under the footings by conducting laboratory model tests (Guido et al. 1986; Omar et al. 1993; Das et al.1994; Das and Khing1994; Das and Omar 1994; Yetimoglu et al. 1994; Huang and Menq 1997; Das et al. 1998; Shin et al. 2002; Kumar and Saran 2003; Kumar et al. 2007) .Adams and Collin (1997) conducted large scale model footing tests to study the ultimate bearing capacity on geogrid reinforced soil. The model test results and analysis were done mostly for centric loading and surface footing. Patra et al. (2005), Patra et al. (2006) studied the behavior of eccentric load on strip foundation supported on geogrid reinforced foundation beds. Much research work has not been done in shallow foundations of square footing subjected to eccentric load resting on geogrid reinforced soil. In this project, it is intended to carry out research work on shallow foundations subjected to eccentric load supported by geogrid reinforced sand.

Guido et al. (1986) presented a comparison of the results of laboratory model tests used to study the bearing capacity of geogrid and geotextile reinforced earth slabs. For both geogrid and geotextiles, after an optimum number of layers or width of reinforcement, the bearing capacity did not increase. The bearing capacity was largest for those geogrid and geotextile reinforced

earth slabs where the first layer was closest to the footing and the spacing between the layers was the smallest. Bearing capacity increased directly with increasing reinforcement tensile strength for the geotextile; and for the geogrid, aperture size and reinforcement tensile strength must be looked at simultaneously.

Yeo et al. (1992) presented laboratory model test results for permanent settlement of a shallow square foundation supported by geogrid-reinforced sand and subjected to cyclic loading. Tests were conducted with only one type of geogrid and at one relative density of compaction of sand. Based on the model test results, the nature of variation of the permanent settlement of the foundation with the intensity of the static loading and the amplitude of the cyclic load intensity are presented in a non-dimensional form.

Omar et al. (1993) performed laboratory model test to study the ultimate bearing capacity of strip and square foundations supported by sand reinforced with geogrid layers. Based on the model test results, the critical depth of reinforcement and the dimensions of the geogrid layers for mobilizing the maximum bearing-capacity ratio have been determined and compared. From this experiment they concluded that for development of maximum bearing capacity the effective depth of reinforcement are about 2B for strip footings and 1.4B for square footings and the maximum width of reinforcement layers for optimum mobilization of maximum bearing capacity ratio is 8B for strip footings and 4.5B for square footings.

Das and Omar (1993) carried out laboratory model test to determine the ultimate bearing capacity of surface strip foundations on geogrid-reinforced sand and unreinforced sand. A fine uniform sand and one type of geogrid were used for the tests. The analysis of the test results revealed that the bearing capacity ratio of the sand-geogrid system decreased with an increase in foundation width. .

Yetimoglu et al. (1994) investigated the bearing capacity of rectangular footings on geogrid-reinforced sand by performing laboratory model tests as well as finite-element analyses. For single-layer reinforced sand, 0.3B is an optimum embedment depth for the first reinforcement layer and for multilayer 0.25B is the embedment depth at which the bearing capacity is the highest. For multilayer reinforced sand, the optimum vertical spacing of reinforcement layers lies in between 0.2 to 0.4B and the effective zone lies approximately within 1.5B from both the base and edges of the footing. The bearing capacity of reinforced sand increase with reinforcement layer number and reinforcement size when the reinforcement was placed within a certain effective zone. In addition the analysis indicates that increasing reinforcement stiffness beyond a certain value would not being further increase in the bearing capacity.

Das et al. (1994) presented laboratory model test results for the ultimate bearing capacity of a strip foundation supported by geogrid-reinforced sand and saturated clay. One type of geogrid was used for all the tests. On the basis of the model test results, the optimum depth and width of reinforcing layers and the optimum depth of the location of the first layer of the geogrid in sand and saturated clay were determined and compared.

Huang and Menq (1997) performed quantitative evaluations on two failure mechanisms (i.e. deep footing and wide slab mechanisms), that dominates the bearing capacity characteristics of sandy ground reinforced with horizontal reinforcing layers. The improvement contributed by reinforcement, creating a quasi-rigid, wide earth slab immediately under the footing to the bearing capacity is analyzed. The results of a total of 105 model tests are analyzed using calibrated internal friction angle of sand and an experimentally verified failure mechanism in reinforced sandy ground, namely, the deep footing mechanism. Based on this study to determine

the ultimate bearing capacity of a strip surface foundation on reinforced sand based on wide-slab mechanism can be expressed as

$$q_{u(R)} = 0.5(B + \Delta B)\gamma N_{\gamma} + \gamma d N_q \tag{2.15}$$

$$d = u + (N - 1)h \tag{2.16}$$

$$\Delta B = 2d \tan\beta \tag{2.17}$$

$$\tan\beta = 0.68 - 2.071\left(\frac{h}{B}\right) + 0.743(CR) + 0.03\left(\frac{b}{B}\right) \tag{2.18}$$

Where, B = foundation width, d = depth of Reinforcement measured from the bottom of the foundation, u = Location of the top layer of reinforcement measured from the bottom of the foundation, N = number of reinforcement layer, h=vertical distance between two consecutive layers, CR = cover ratio (w/W), b = width of reinforcement layer, w = width of longitudinal ribs, W = Center-to-center of the longitudinal ribs. N_{γ}, $N_q$are bearing capacity factors. $tan\beta$ = load-spreading angle, ΔB = increase of footing width at depth d due to wide-slab effect.

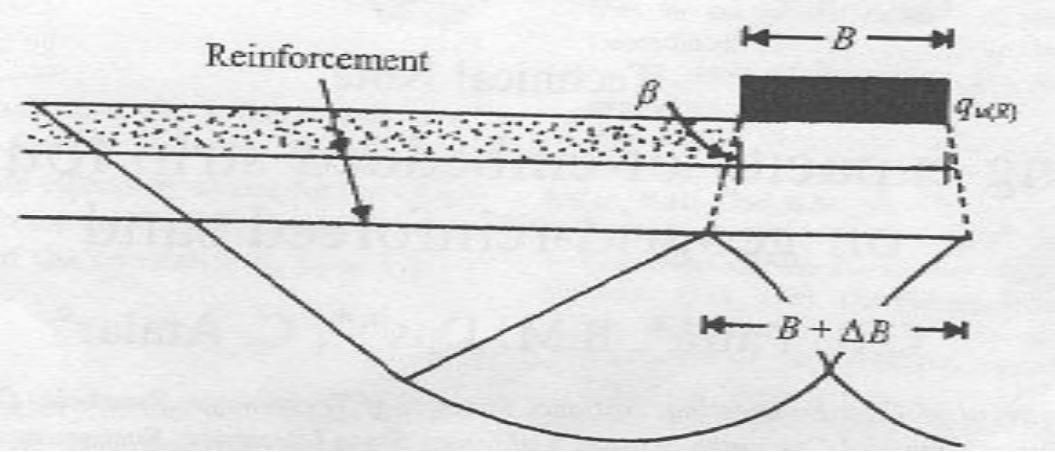

Figure 2.2: Wide-slab failure mechanism in reinforced sand supporting a strip foundation (source Huang and Menq, 1997)

Kumar and Saran (2003) performed laboratory model tests on closely spaced strip and square footings on geogrid-reinforced sand. From the analysis of test results it was shown that the interference effects on bearing capacity and settlement of closely spaced square footings on reinforced sand were almost insignificant in comparison to those on isolated footings on reinforced sand; whereas a significant improvement in the tilt of adjacent square footings has been observed by providing continuous reinforcement layers in the foundation soil under the closely spaced footings.

Patra et al. (2005) conducted laboratory model tests on a strip foundation supported by multi-layered geogrid-reinforced sand. The depth of embedment of the model foundation d_f is varied from zero to B (width of foundation). Only one type of geogrid and one variety of sand at one relative density were used. The ultimate bearing capacity obtained from the model test program is compared with the theory proposed by Huang and Menq (1997). Based on the present tests, it appears that the theory provides a conservative prediction of the ultimate bearing capacity.

Patra et al. (2006) conducted laboratory model tests on strip foundation supported by geogrid-reinforced sand subjected to eccentric load. Based on the laboratory test results, an empirical relationship called reduction factor is suggested that correlates the ratio of the ultimate bearing capacity of an eccentrically loaded foundation with that for a foundation where the load is applied centrally. The reduction factor is a function of d_f / B and e/B.

$$\frac{q_{uR(e)}}{q_{uR}} = 1 - R_{KR} \tag{2.19}$$

$$R_{KR} = 4.97\left(\frac{d_f}{B}\right)^{-0.12}\left(\frac{e}{B}\right)^{1.21} \tag{2.20}$$

$q_{uR\,(e)}$ = ultimate bearing capacity due to eccentric loading, $q_{uR\,(e=0)}$ = ultimate bearing capacity due to centric loading. R_{KR} = reduction factor for geogrid-reinforced sand.

$d_f = D_f + d$

Where, d = depth of Reinforcement measured from the bottom of the foundation, D_f = depth of foundation.

CHAPTER 3

EXPERIMENTAL WORK AND METHODOLOGY

3.1 Introduction

The experimental program was designed to study the bearing capacity of eccentrically loaded square footing on multi-layered geogrid reinforced sand bed. For this purpose, the laboratory model tests were conducted on square footings in one densities (i.e. dense), load eccentricity e was varied from 0 to 0.15B (B = width of strip footing), number of geogrid layer are varied (i.e. N = 2, 3, 4). All tests have been conducted in surface case only. The ultimate bearing capacity was interpreted from each test and analyzed.

3.2 Materials Used in the tests

In this chapter two materials are used (sand and geogrids)

3.2.1 Sand

Sample collection

The sand used in the experimental program was collected from the river bed of a nearby Koel river. It is made free from roots; organic matters etc. by washing and cleaning. The above sample was then oven dried and properly sieved by passing through IS 710 micron and retained at IS 300 micron sieves to get the required grading. Dry sand is used as soil medium for the test as it does not include the effect of moisture and hence the apparent cohesion associated with it.

Characteristics of sand

The geotechnical properties of the sand used is given in Table 3.1. The grain size distribution curve is plotted in Figure 3.1. All the tests were conducted in one density (dense) with relative densities of 69%. The average unit weight of relative densities is 14.32kN/m^3. The friction angle at relative densities of 69% is 40.8^0 which are found out from direct shear tests.

Table 3.1. Geotechnical property of sand

Property	**Value**
Specific gravity *(G)*	2.64
Effective particle size (*D10*)	0.325mm
Mean particle size (*D50*)	0.46mm
Uniformity Coefficient (*Cu*)	1.45
Coefficient of Curvature (*Cc*)	1.15
Working dry density (γ_d)	14.32 KN/m^3
Maximum unit weight($\gamma_{d(max)}$)	15.19 KN/m^3
Minimum unit weight ($\gamma_{d(min)}$)	12.90 KN/m^3

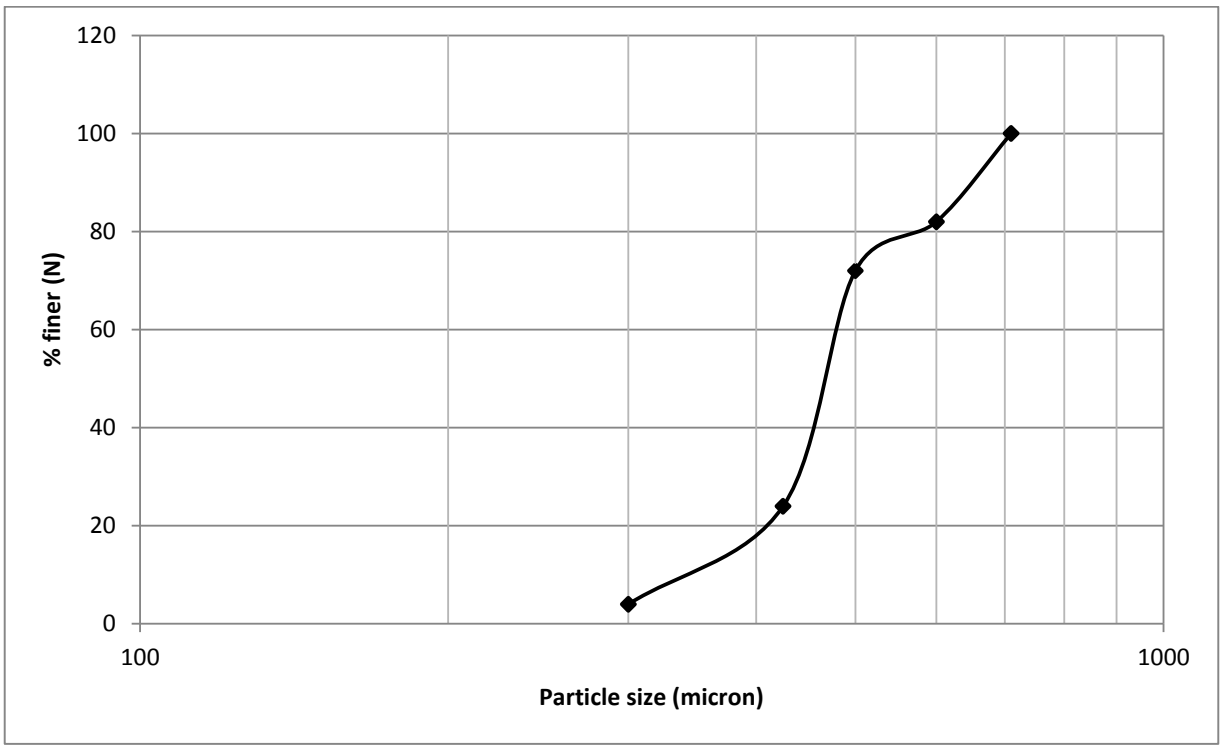

Figure 3.1: Grain-size distribution curve of sand

3.2.2 Geogrid

Biaxial geogrid (SS20) is used for the present tests. Geogrid layers are placed inside the sand layer at desired values of *u/B* and *h/B.* The physical and mechanical properties of the geogrids as listed by the manufacturer are given below-:

Table 3.2: Physical properties of the geogrid:

Parameters	**Quantity**
Polymer	Polypropylene Pp
Tensile strength at 2% strain	7 *KN/m*
Tensile strength at 5% strain	14 *KN/m*
Aperture size	39*39 mm
Aperture shape	square
Rib thickness	1.1 mm
Junction strength	95%

3.3 Test tank

A test tank of inside dimension 1.0m (length) 0.504m (width) 0.655m (height) is used. The two length sides of the tank were made of 12mm thick high strength fiberglass. The two width sides of tank are made up of mild steel of 8mm thickness. Scales are fitted on the middle of the four internal walls of the box so that it will be easier in maintaining the required density accurately. All four sides of the tank are braced to avoid bulging during testing. The following considerations are taken into account while deciding the dimension of the tank. As per provision of IS 1888-1962 the width of the test pit should not be less than 5 times the width of the test plate, so that the failure zones are freely developed without any interference from sides. Chumar

(1972) has suggested that in case of cohesionless soil the maximum extension of failure zone is 2.5B to the both sides and 3B below the footing. By adopting the above tank size for the model footing (10cm x 10cm), it is ensured that the failure zones are fully and freely developed without any interference from the sides and bottom of the tank.

3.4 Equipments used

- Load transferring shaft
- Model footing
- Proving ring
- Dial gauge

a) Model footing

Model footing used for laboratory tests are made of mild steel plate of sizes $10cm \times 10cm \times 3cm.$ One footing is meant for centroidal loading and other three are meant for eccentrical loading, the eccentricity being 0.05B, 0.1B, 0.15B respectively. The bottom of the footing was made rough by applying epoxy glue and then rolling the model footing over sand to give the effect of roughness of actual foundation. Circular depressions accommodating steel balls are made on the footings at proper points so that the loading pattern i.e. centroidal and eccentrical mode can be maintained. The load is transmitted from the loading pad to the footing through the combination of load transferring through spindle and steel ball.

b) Proving ring

Three proving ring are used of 5 KN, 10 KN, 20 KN whose least count are 6.67N, 10.471N, 24.242N respectively.

c) Dial gauge

Two dial gauges of following specifications are used during the tests.

Least count 0.01mm, Range 50 mm. The dial gauges are kept on the top portion of the longitudinal sides of the box because the top portion of the entire box has steel strip welded wide enough to accommodate the magnetic base of the dial gauge. The dial gauge needles are placed over the footing attached with the load transferring column. As the load is applied settlement occurs which is recorded by two dial gauges. The average of the two dial gauge readings is taken as required settlement in mm.

3.5 Sample preparation

First the internal dimensions of the tank are measured accurately and volume for the required thick layer (i.e. 2.5 cm) is calculated. After fixing a density, at which all the tests are to be done by we can calculate the weight of sand needed for that particular thickness of sand layer. Here the density to be maintained is 1.46 gm /cc and the layer of thickness is 2.5 cm. It is found that for maintaining the required density in 2.5 cm layer, required weight is 18.432 kg. The box is filled by sand using sand raining technique. Sand was poured into the test tank in layers of 2.5cm from a fixed height by raining technique to achieve the desired average unit weight of compaction. The height of fall was fixed by making several trials in the test tank prior to the model test to achieve the desired unit weight.

For the test without reinforcement footing is placed on the surface. For the application of eccentrically vertical loads to the footing, groove have been made on the top surface of footing at varying distance from the center of the footing as per the required eccentricity to be maintained.

For the test with reinforcement the first geogrid layer is placed at a depth of 0.35B from the base of the footing, the other subsequent layer of geogrid being placed at equal spacing of 0.25B. After putting the geogrids, small weight are placed on them to keep the geogrids in position and then the required weight of sand is poured over it using sand raining technique.

3.6 Test procedure

- After filling the tank surface to a desired height, the filled surface is leveled and the footing is placed on a predetermined alignment such that the load transferred vertically to the footing.
- Then placing the steel ball over the circular groove of the footing, the load transferring shaft is placed over it, through which the load is transferred to the footing vertically.
- Two dial gauges are placed over the footing on the opposite sides of the spindle. Then the initial readings of two dial gauges are noted.
- The load is then applied and the footing is allowed to settle under the applied load. Each load increment is maintained till the footing settlement get stabilized which is measured from the two dial gauge readings.
- The processes of load application is continued till there is failure of foundation soil due to sudden excessive settlement or up to 25mm settlement occur which can be observed in the proving ring of the jack where the load taken by the footing get decreased continuously.
- On completion of the load test, the equipments are removed, tank emptied and the tank again filled for the next set of load test.

Figure 3.2: Photographic image of sand sample at the start of experiment

Figure 3.3: Placing of geogrid

3.7 Geometric parameters

A square foundation of width 'B' supported by geogrid-reinforced sand. There are four layers of geogrid, each having a width 'b'. The top layer of geogrid is located at a depth u from the bottom of the foundation. The vertical distance between consecutive layers of geogrid is 'h'. The primary aim has been to evaluate the following parameters in a dimensional form, from which the most beneficial effect of geogrid reinforcement can be derived. The reinforcement depth below the bottom of the foundation can be expressed as

$$d = u + (N-1)h$$

The magnitude of the bearing capacity for a given foundation, sand and geogrid will depend on *e/B, d/B.* In order to conduct a model tests with geogrid reinforcement in sand, it is important to decide the magnitude of *u/B* and *b/B* to derive maximum benefit in increasing the ultimate bearing capacity. Omar et al. (1992) was conducted a test for model strip and square foundation to decide the magnitude of *u/B.* By conducting model tests on surface foundation (D_f = 0) supported by sand with multiple layer of reinforcement, which is shown by several previous investigators (Guido et al. 1987, Akhinmusuru and Akinbolande 1981, Yetimogulu et al. 1994, Shin and Das 1999) for a given values of *h/B, d/B* and *b/B.* the magnitude of BCR_u increases with *(u/B)* and attains a maximum value at $(u/B)_{cr}$. For *(u/B)* > $(u/B)_{cr}$, the magnitude of BCR_u decreases. By compiling several test results Shin and Das (1999) determined that $(u/B)_{cr}$ for strip foundations can vary between 0.25 and 0.5. Omar et al. (1993c) determined that $(b/B)_{cr}$ 8 for strip footing and 4.5 for square footing. Guido et al. (1987) determined that $(h/B)_{cr}$ should be lie in between 0.25 to 0.4. Keeping all these factors in mind it is decided to adopt the following parameters for the present tests.

u/B = 0.35, *h/B* = 0.25, *b/B* = 4.5

3.8 Model test series

Table: 3.3: The sequence of the model test series (For unreinforced case)

Test series	D_f / B	B/ L	e / B
1-4	0	1	0,0.05,0.1,0.15

Table: 3.4: The sequence of the model test series (For reinforced case)

Test series	D_f / B	B/ L	e / B	N
5-8	0	1	0,0.05,0.1,0.15	0.6,0.85,1.1
9-12	0	1	0,0.05,0.1,0.15	0.6,0.85,1.1
13-16	0	1	0,0.05,0.1,0.15	0.6,0.85,1.1

CHAPTER 4

EXPERIMENTAL RESULTS AND ANALYSIS

4.1 Introduction

The load tests for surface square footings of dimension (10cmx10cm) have been conducted in the laboratory with load eccentricity varying from 0 to 0.15*B* with an increment of 0.05*B* in unreinforced sand and with geogrid SS20 as reinforcement in 2, 3 and 4 number of layers in geogrid reinforced sand. The results of each load tests were plotted in arithmetic graph paper in the form of load-settlement curve. The analysis of the test results is discussed in detail in the following paragraphs.

4.2 Ultimate bearing capacity for unreinforced sand (test series A*)*

4.2.1 Model test results

The combined graph showing load-settlement curve is shown in Figure 4.1. From Figure 4.1 it is seen that as the eccentricity ratio (*e*/*B*) increases, the load carrying capacity decreases as well as the total settlement decreases. At any load intensity, the increase in settlement is accompanied by increase in eccentricity or at any settlement, the increase in eccentricity is accompanied by decrease in load intensity.

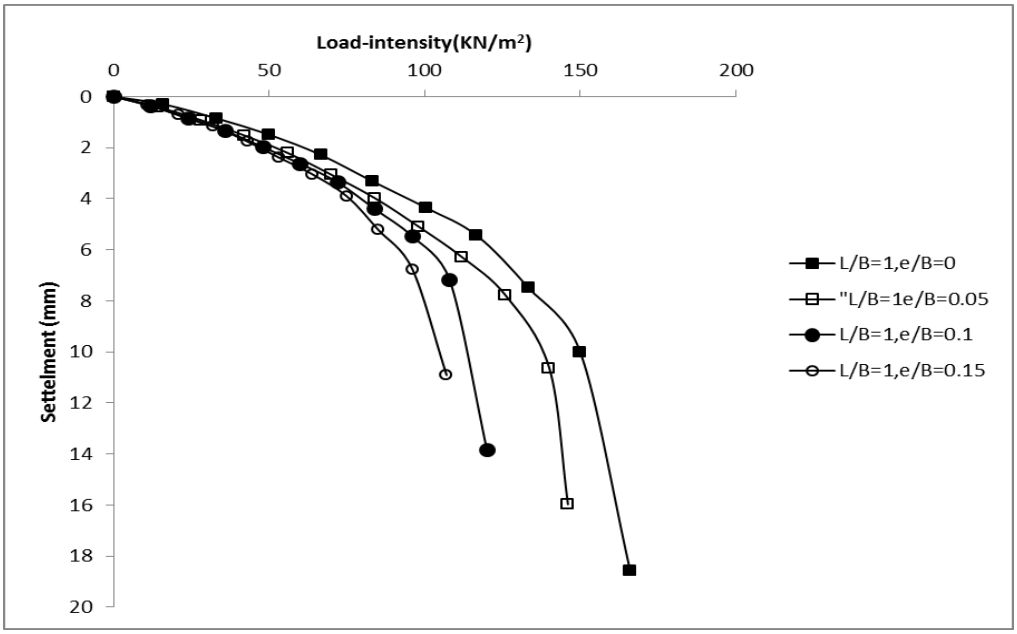

Figure 4.1: Plot of load-settlement curves for various eccentricity ratio in unreinforced sand (Present experimental data)

From the load-settlement curves shown in Figure 4.1, the ultimate bearing capacities are determined for each test are shown in Figure 4.2 along with the theoretical values using well known available theories (Terzaghi, 1943; Meyerhof, 1953; Vesic, 1973; Hansen, (1970) and IS code IS: 6403-1981). It is seen that Meyerhof's theory is in close agreement to those of experimental values obtained, otherwise, the values obtained by experiments is usually higher than those obtained using other theories. The corresponding values are also shown in Table 4.1. It can be seen that experimental bearing capacities for a given D_f /B are significantly higher than those predicted by theory. Investigators like Balla 1962, Bolt 1982, Cichy et al. 1978, Ingra and Baecher 1983, Hartikainen and Zadroga 1994, Milovic 1965, Saran and Agarwal 1991, Shiraishi 1990, and Zadroga 1975 revealed that bearing-capacity model test results which are being carried out in various geotechnical laboratories of shallow footings and strip foundations are, in general, much higher than those calculated by traditional methods

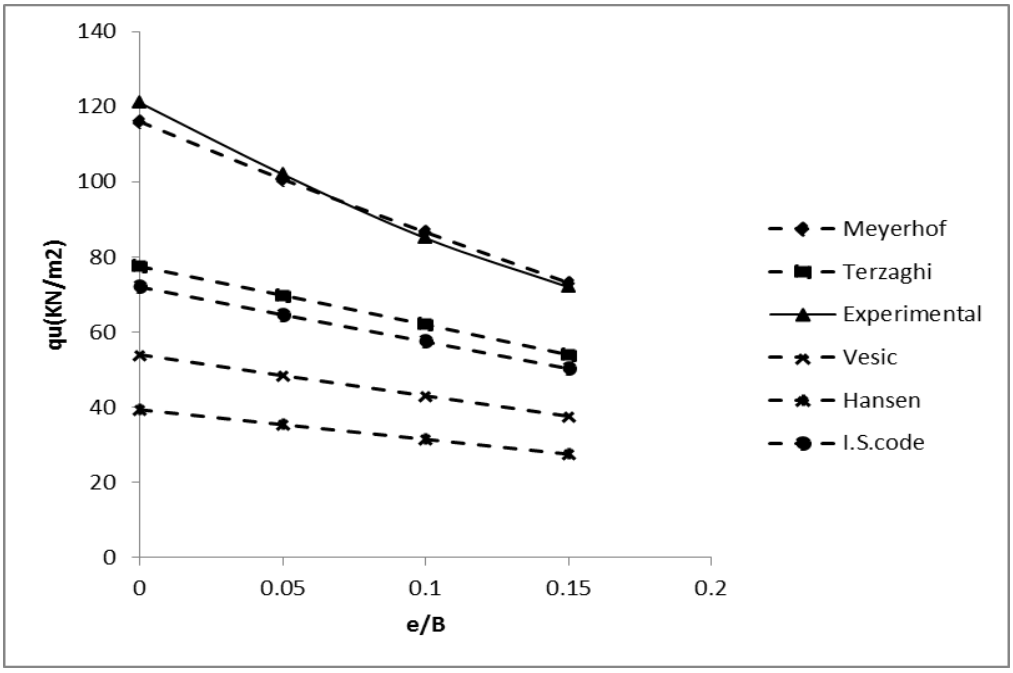

Figure 4.2: Variation of q_u with different e/B

Table 4.1 Calculated values of ultimate bearing capacity q_u by Meyerhof (1951), Terzaghi (1943), Vesic (1973), Hansen (1970), and IS code IS: 6403-1981

Sl no	N	e/B	D_f/B	Present experiment q_u (KN/m^2)	Meyrhof q_u (KN/m^2) ϕ=40.8	Terzaghi q_u (KN/m^2) ϕ=40.8	Vesic q_u (KN/m^2) ϕ=40.8	I.S. code q_u (KN/m^2) ϕ=40.8	Hansen q_u (KN/m^2) ϕ=40.8
1	0	0	0	121	116	77.47	54	72	39.37
2	0	0.05	0	102	100.67	69.82	48	64.62	35.4
3	0	0.1	0	85	86.59	62	43	57.46	31.47
4	0	0.15	0	72	73.16	54	37.65	50.3	27.55

DeBeer (1965) compiled several bearing capacity test results which are shown in Figure 4.3 as a plot of N_γ vs. γB. The value of N_γ rapidly decreases with the increase in γB. In addition, DeBeer (1965) compared the variation of N_γ obtained from small scale laboratory and large scale field test results, and these are given in Figure 4.4.

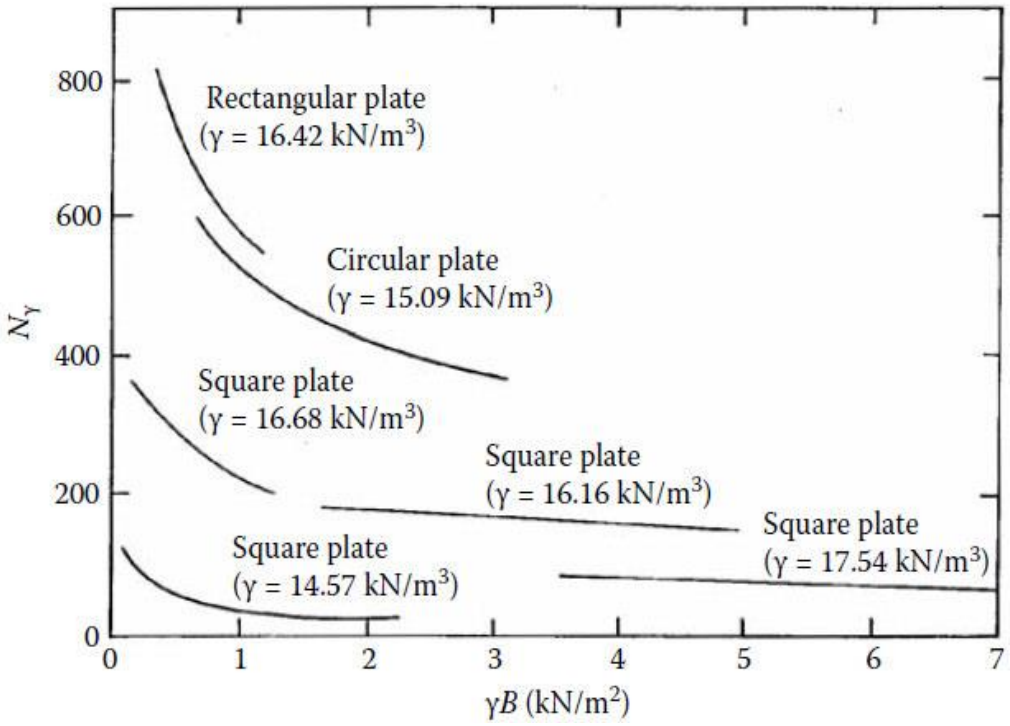

Figure 4.3: Variation of N_γ with γB (adapted after DeBeer, 1965)

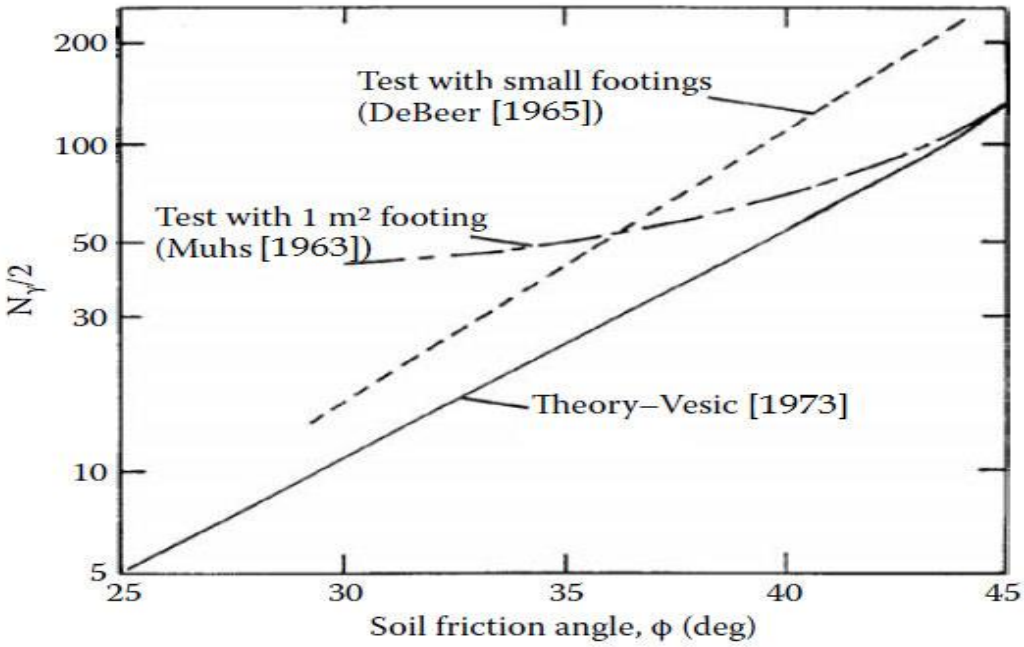

Figure 4.4: Comparison of N_γ obtained from tests with small footings and large footings of 1m² area on sand (adapted after DeBeer, 1965).

4.3 Ultimate bearing capacity for geogrid reinforced sand (test series B)

4.3.1 Model test results

The load tests have been conducted for surface square foundation (10cm x 10cm) supported by multi-layered geogrid reinforcement (i.e. d/B = 0.6, 0.85, 1.1) with load eccentricity e/B (=0.05, 0.1 and 0.15). The results of load intensity and corresponding settlement of each test have been plotted in arithmetic graph paper. The ultimate bearing capacity in each case has been determined by double tangent intersection method.

The combined load-settlement graphs are shown in Figures 4.5, 4.6, and 4.7 to quantify the effect of eccentricity at any number of reinforcement layer (i.e. N=2, 3 or 4). From Figures 4.5 through 4.7 it is seen that with any number of geogrid layers, as the eccentricity increases, the ultimate bearing capacity decreases. Furthermore, it is seen that with any number of geogrid layers, at any bearing pressure the settlement of footing increases with increase in eccentricity. Similarly, it is

also seen that at any number of geogrid layers, bearing pressure at any settlement level decrease with increase in eccentricity of the load.

The bearing capacity of footing increases with the increase in number of geogrid layers and decreases with different eccentricity ratio.

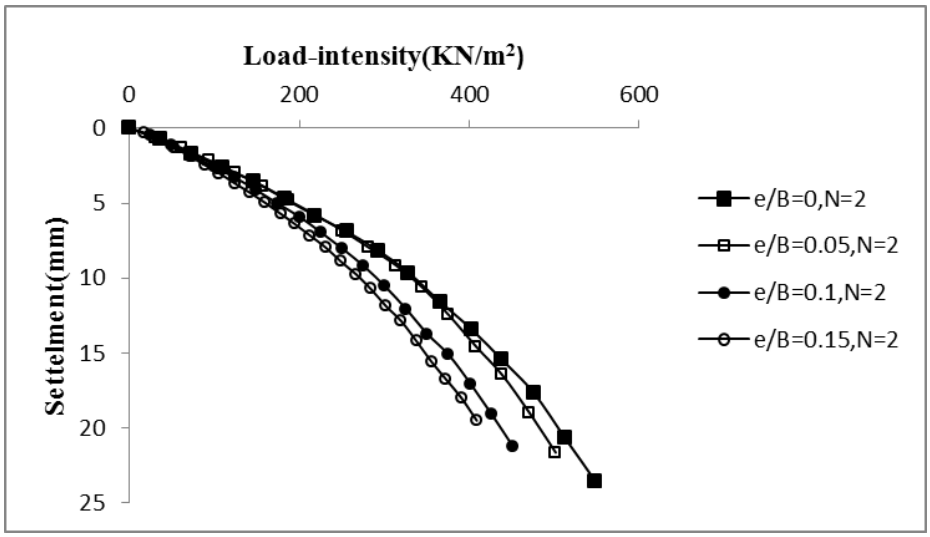

Figure 4.5: Variation of load-settlement curve with depth of reinforcement layer *N*=2

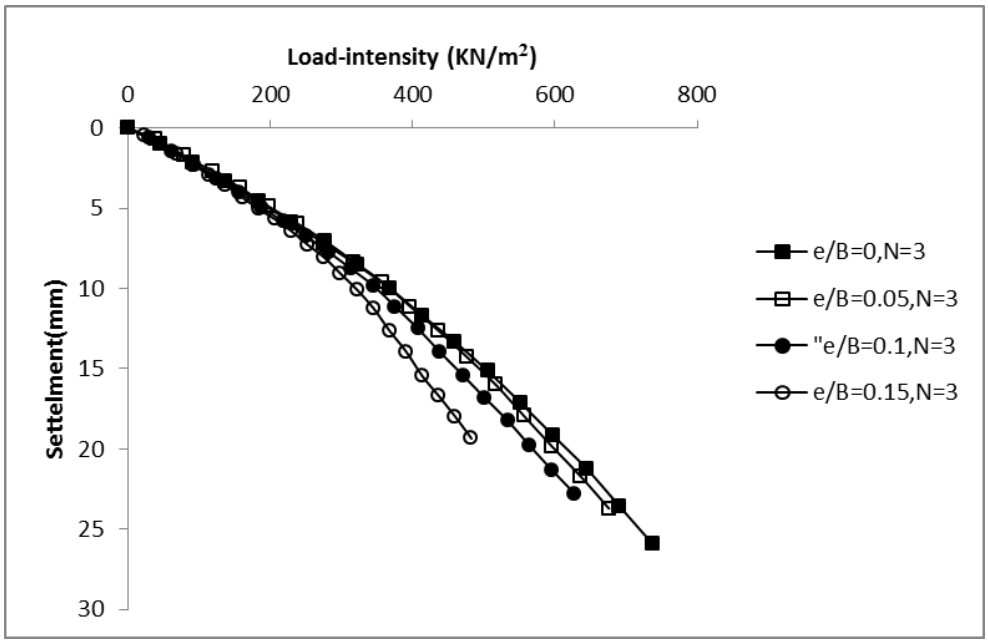

Figure 4.6: Variation of load-settlement curve with depth of reinforcement layer *N*=3

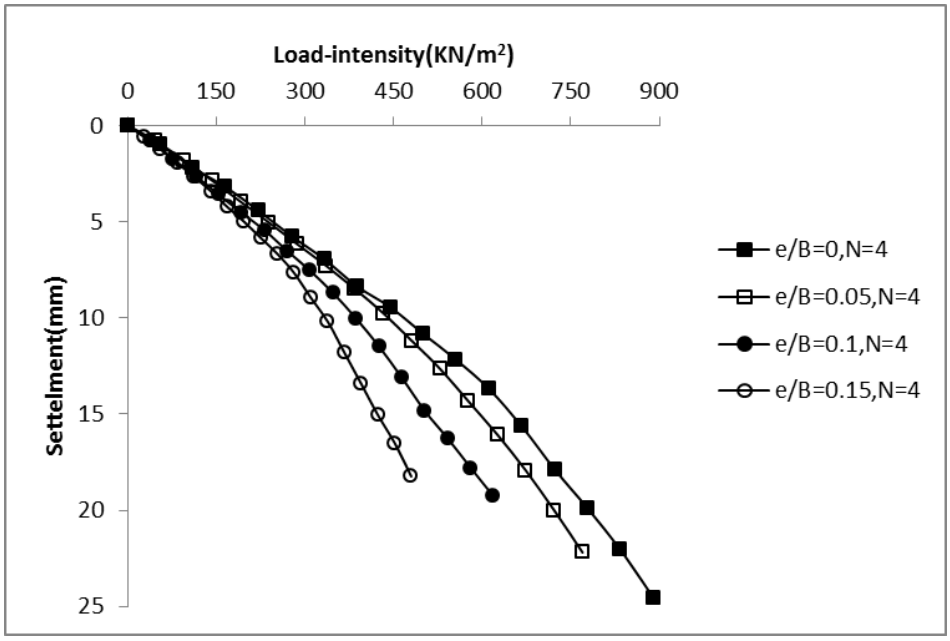

Figure 4.7: Variation of load-settlement curve with depth of reinforcement layer *N*=4

The load-settlement curves have been shown in Figures 4.8 through 4.11 to show the effect of number of geogrid layers on the load bearing capacity and settlement at any eccentricity of load application. It is seen that at any eccentricity, the bearing pressure increases with increase in the number of geogrid layers at any level of settlement. Similarly at any level of bearing pressure, the settlement of the footing decreases with increase in the number of reinforcing layer.

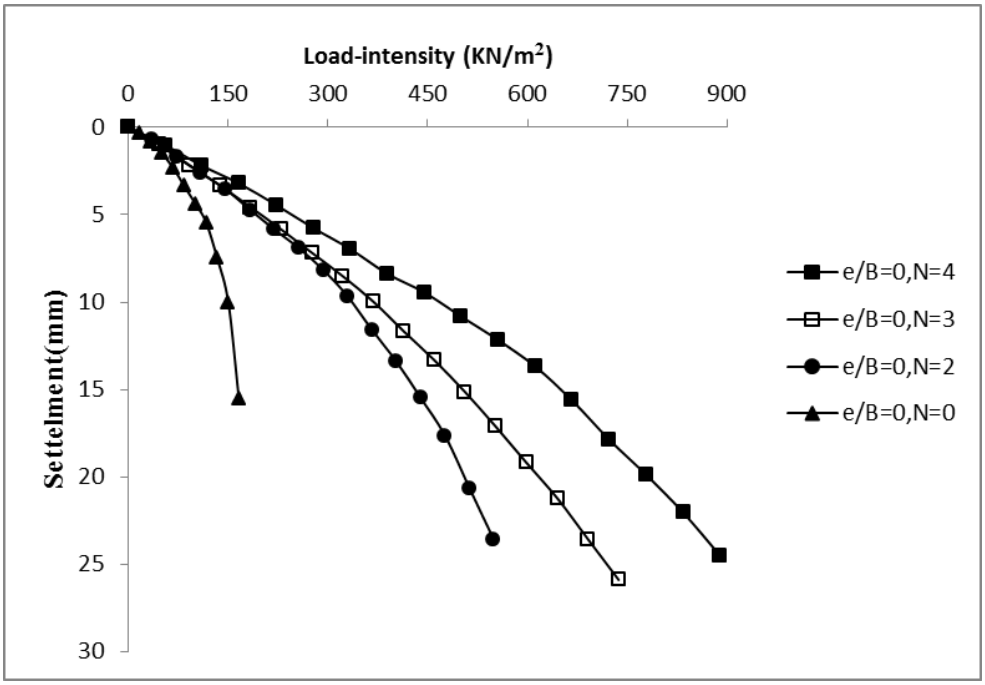

Figure 4.8: Variation of load-settlement curve with surface case (*e/B*=0)

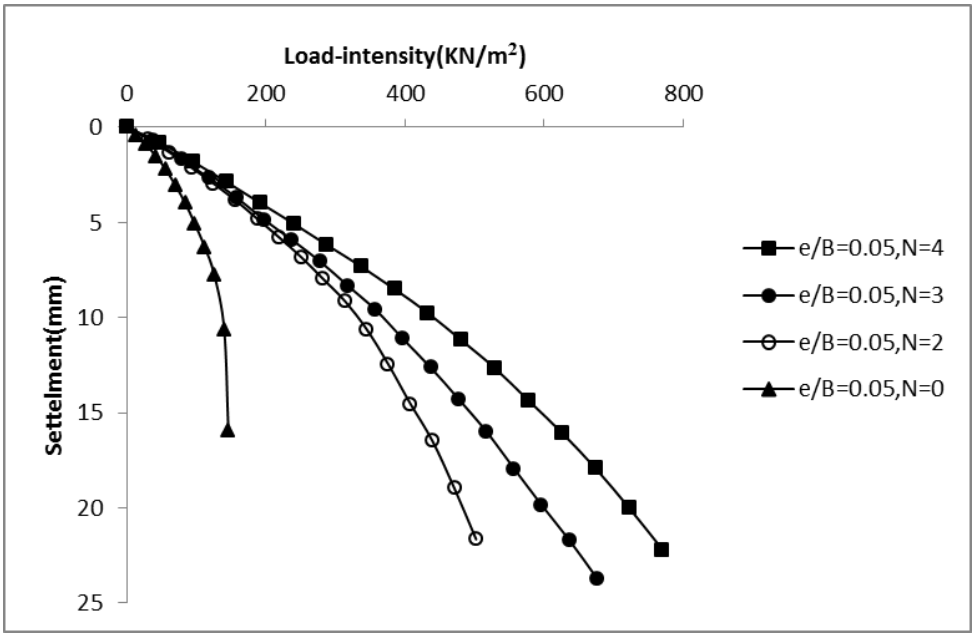

Figure 4.9: Variation of load-settlement curve with surface case (*e/B*=0.05)

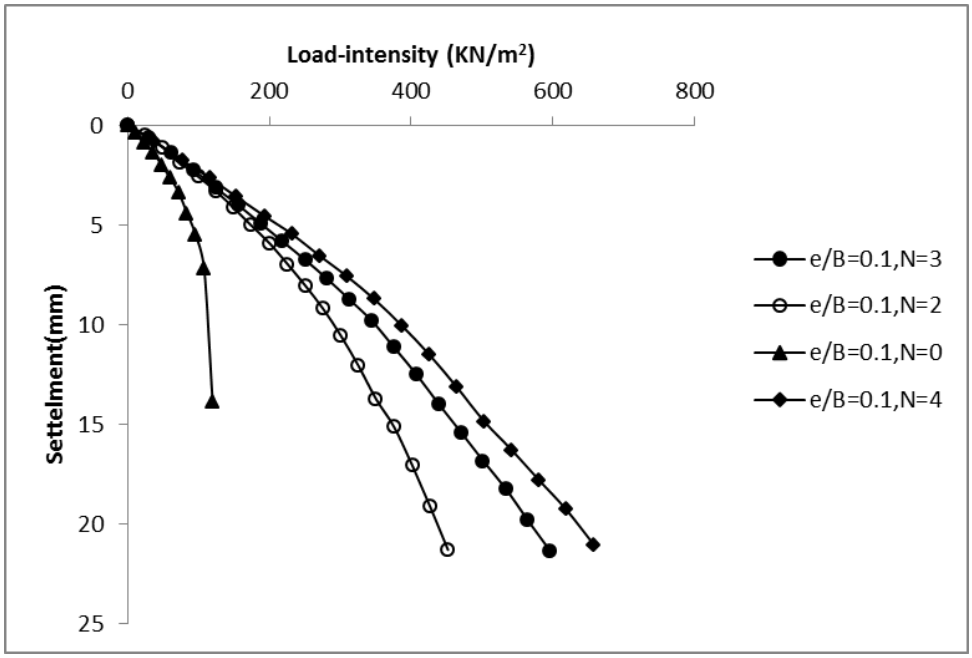

Figure 4.10: Variation of load- settlement curve with surface case (*e/B*=0.1)

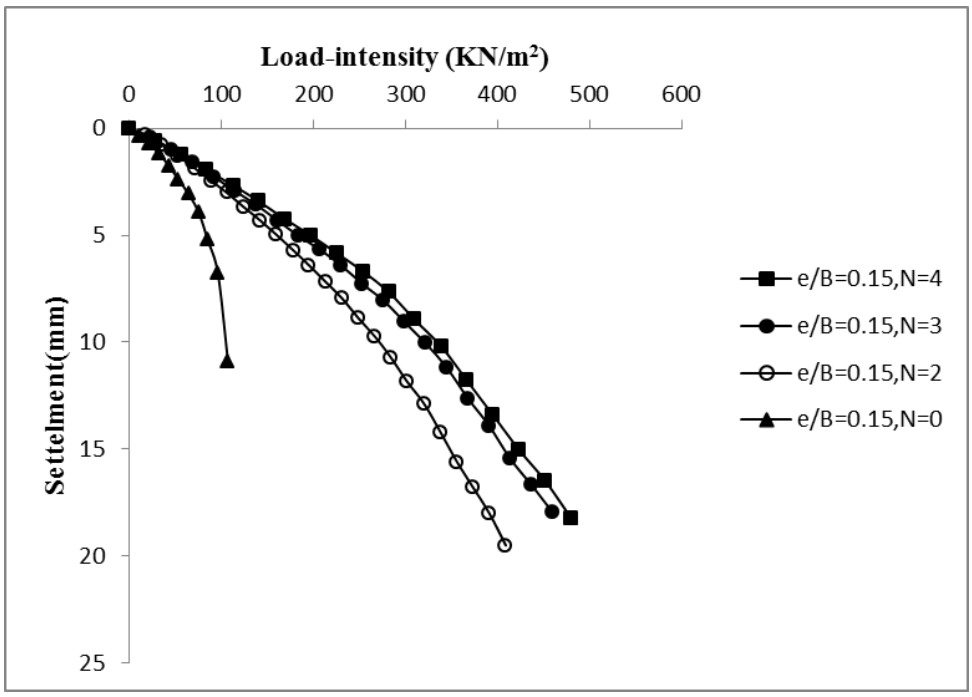

Figure 4.11: Variation of load-settlement curve with surface case (*e/B*=0.15)

4.3.2 Analysis of test results

A reliable procedure for estimating the ultimate bearing capacity under centric loading for a strip foundation supported by geogrid reinforced sand is yet to be developed. Takemura et al. (1992) conducted several centrifuge tests for surface foundation to determine the ultimate bearing capacity of a strip foundation on geogrid reinforced sand. Based on the model tests they concluded that, just before load intensity reached its peak, a rigid soil block is formed under the foundation, and this block behaves as if it were an embedded foundation (Figure 4.12). The ultimate bearing capacity without depth factor can conservatively be given as

$$q_{uR} = d\gamma N_q + 1/2\,\gamma B N_\gamma \tag{4.1}$$

Where, q_{uR} = Ultimate bearing capacity on geogrid-reinforced sand, b = width of reinforceme (4.6)

layer, d = depth of Reinforcement measured from the bottom of the foundation,

$$d = u + (N-1)\,h \tag{4.2}$$

(4.6)

N = number of reinforcement layer; h= vertical distance between two consecutive laye.s, u = location of the top layer of reinforcement measured from the bottom of the foundation.

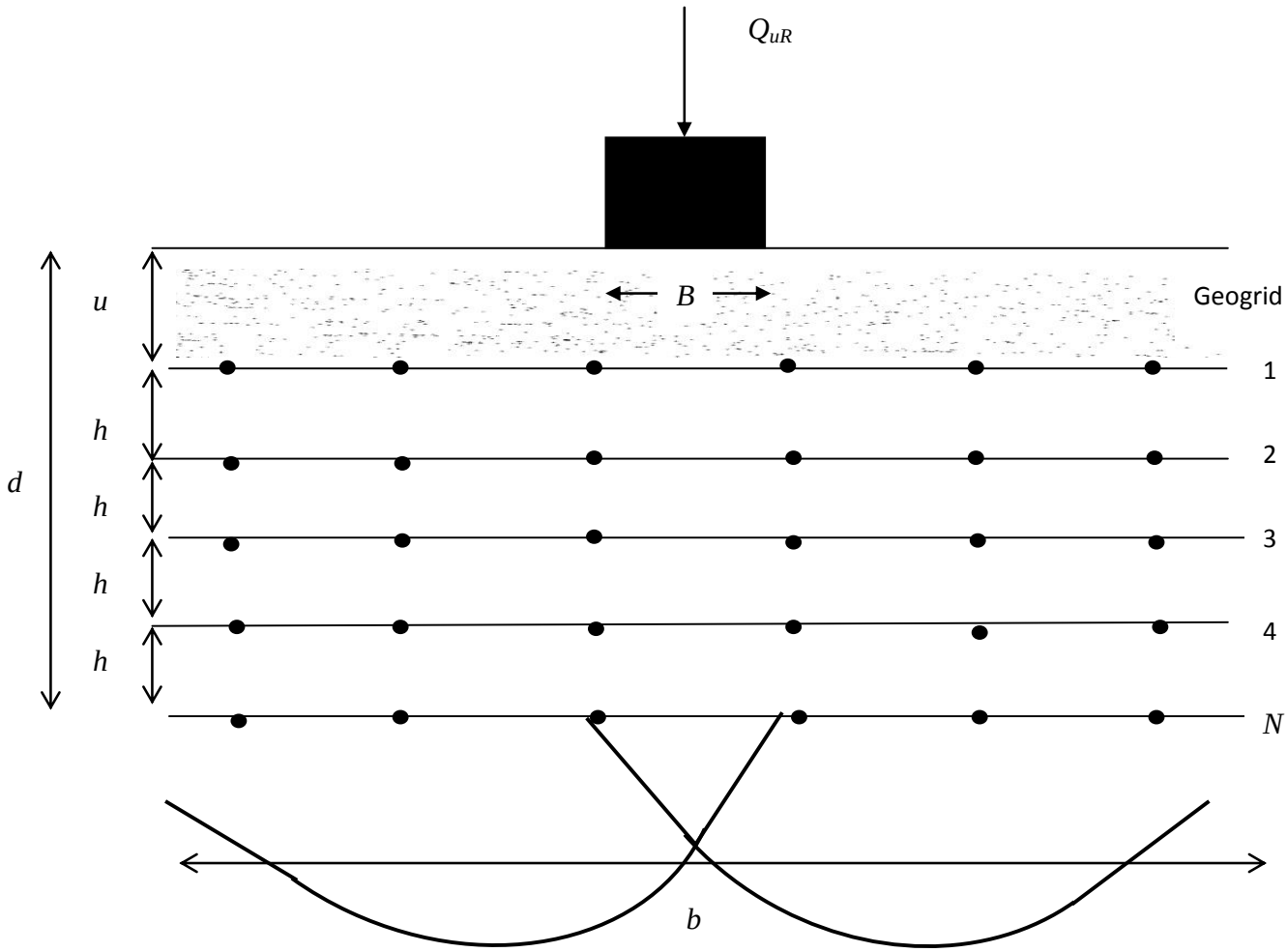

Figure 4.12: Assumed failure mode under a centrally loaded surface square foundation over geogrid-reinforced sand (Source Takemura et al. 1992)

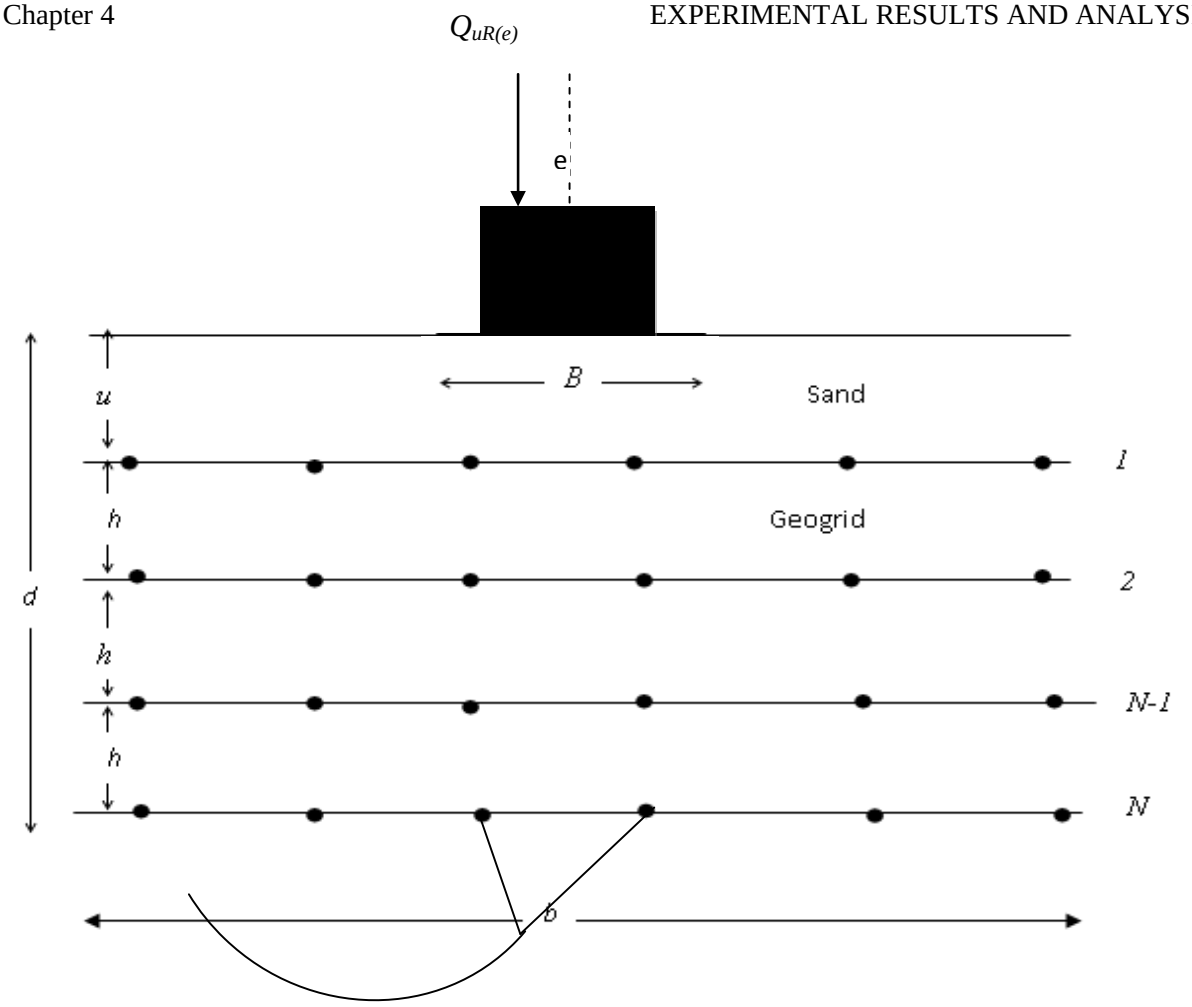

Figure 4.13: Assumed failure mode under an eccentrically loaded square foundation on geogrid-reinforced sand

Assuming the failure mechanism under centric load as shown in Figure 4.12 to be correct, it appears that the ultimate bearing capacity due to eccentric loading (Figure 4.13) may be expressed in a form similar to Eq. 2.9.

$$\frac{q_{uR(e)}}{q_{uR}} = 1 - R_{KR} \tag{4.3}$$

(4.6)

$$R_{KR} = 1 - \frac{q_{uR(e)}}{q_{uR}} \tag{4.4}$$

(4.6)

Where, $q_{uR(e)}$ = Ultimate bearing capacity due to eccentric loading; q_{uR} = Ultimate bearing capacity due to centric loading; R_{KR} = Reduction factor

In Figure 4.13, $Q_{uR(e)}$ is the ultimate load per unit length of the foundation with a load eccentricity *e* and d_f is the depth of reinforcement layer below the bottom of the foundation.

$$d_f = d$$

The reduction factor may be expressed as

$$R_{KR} = \alpha_1 \left(\frac{d_f}{B} \right)^{\alpha_2} \left(\frac{e}{B} \right)^{\alpha_3} \tag{4.5}$$

(4.6)

Here $\alpha_1, \alpha_2, \alpha_3$ are constants.

The purpose of this thesis is to conduct several laboratory model tests on square foundation over geogrid reinforced sand bed with varying *e/B* and *N* and evaluate the coefficients $\alpha_1, \alpha_2, \alpha_3$ as given in Eq. 4.5

The ultimate load in each case of test series *B* has been determined and presented in Table 4.2 and Figure 4.14. Using experimental ultimate bearing capacities as shown in Figure 4.14, the ratio $\frac{q_{uR(e)}}{q_{uR}}$ has been calculated in each case. The reduction factor $R_{kR} = 1 - \frac{q_{uR(e)}}{q_{uR}}$ in each case is determined and shown in column 6 of Table 4.2. .

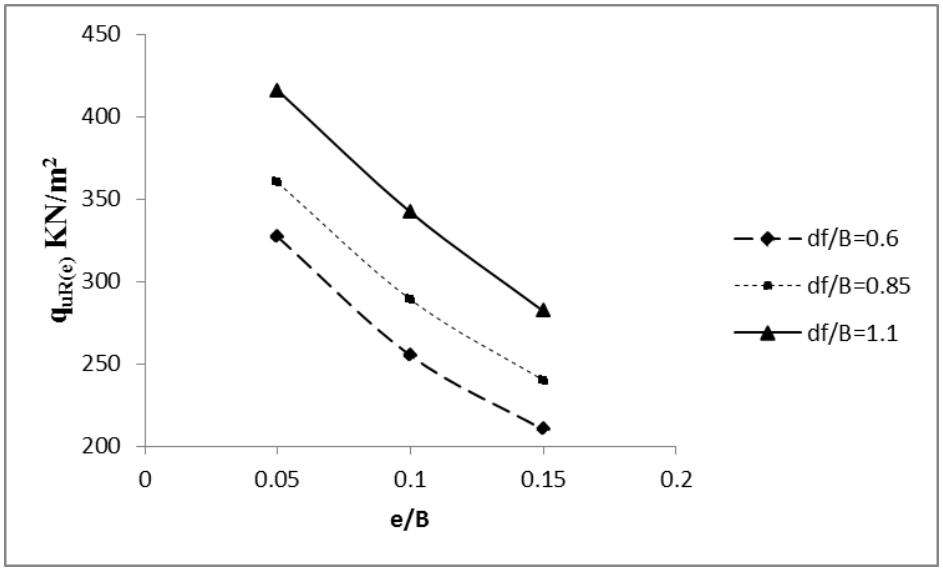

Figure 4.14: Variation of $q_{uR\,(e)}$ versus e/B and d_f/B at D_f/B=0

Table 4.2 Values of reduction factor

$\frac{D_f}{B}$	N	$\frac{e}{B}$	$(q_u)_{experimentally}$	$\frac{q_{uR(e)}}{q_{uR}}$	$R_{KR}=1-\frac{q_{uR(e)}}{q_{uR}}$
0	2	0.05	315kN/m^2	0.875	0.125
0	2	0.1	270kN/m^2	0.75	0.25
0	2	0.15	225 kN/m^2	0.625	0.375
0	3	0.05	340 kN/m^2	0.85	0.15
0	3	0.1	290 kN/m^2	0.725	0.275
0	3	0.15	240 kN/m^2	0.6	0.4
0	4	0.05	421 kN/m^2	0.79	0.21
0	4	0.1	342 kN/m^2	0.64	0.36
0	4	0.15	280 kN/m^2	0.528	0.472

The reduction factor R_{kR} has been shown in Figure 4.15. From this figure it can be seen that for any given d_f /B, the plot of R_{KR} versus e/B is approximately a straight line in a log-log plot. The average value of α_3 is about 0.89

Thus

$$R_{KR} \propto (e/B)^{0.89} \tag{4.6}$$

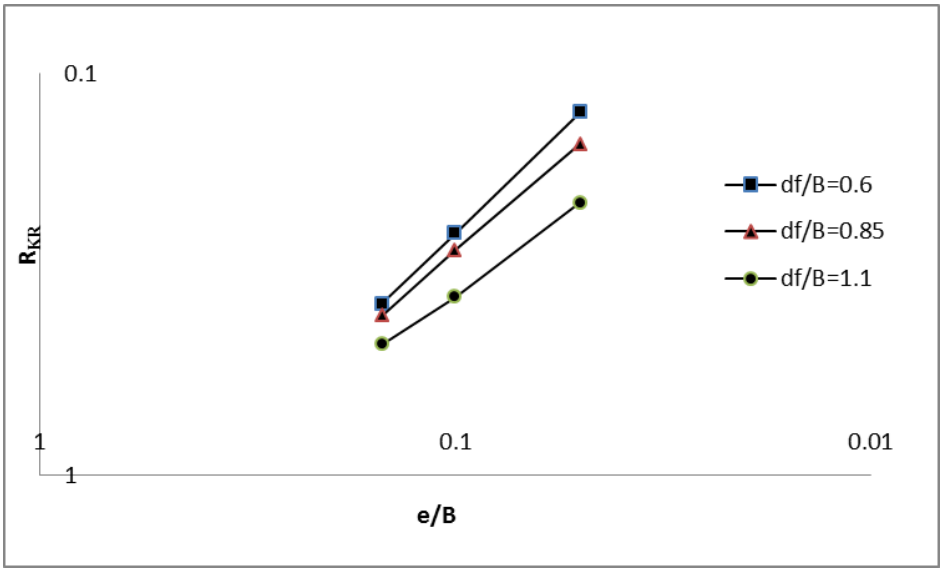

Figure 4.15: Variation of R_{KR} verses e/B at D_f/B=0

Figure 4.16 shows the plots of R_{KR} versus d_f / B for e/B = 0.05, 0.1, 0.15. The slope of the average lines for all e/B values were found out and the value of α_2 is 0.61.

$$R_{KR} \propto (d_f/B)^{0.61} \tag{4.7}$$

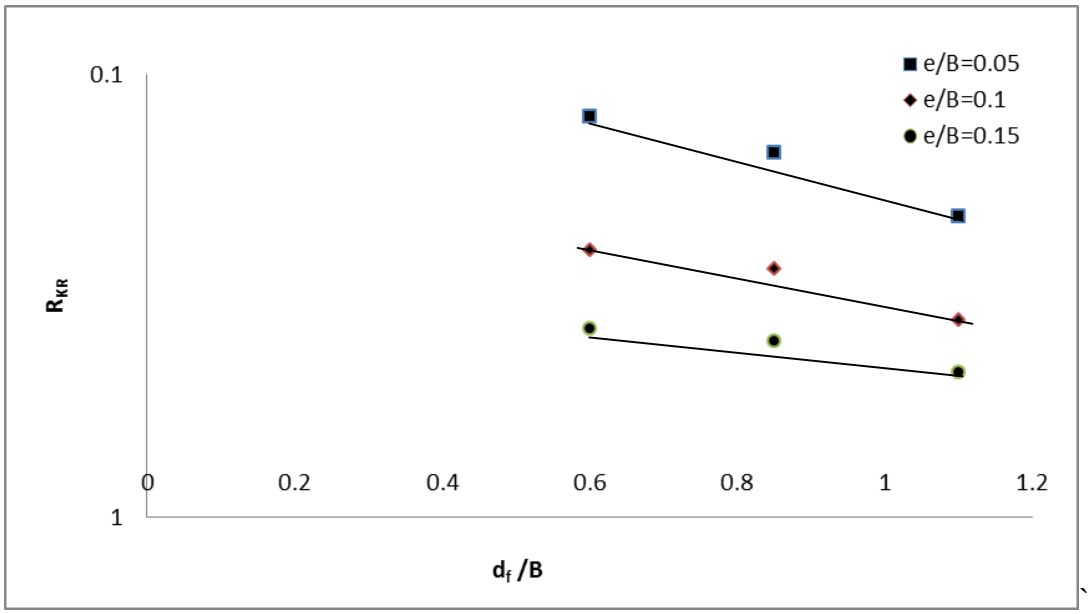

Figure 4.16: Variation of R_{KR} verses d_f/B at D_f/B=0 for e/B=0.05,0.1,0.15

Thus,

$$R_{KR} = \alpha_1 \left(\frac{d_f}{B}\right)^{0.61} \left(\frac{e}{B}\right)^{0.89} \tag{4.8}$$

$$\alpha_1 = \frac{R_{KR}}{(d_f/B)^{0.61}(e/B)^{0.89}} \tag{4.9}$$

Using the average lines for each e/B shown in Figure 4.16 the magnitudes of α_1 were calculated. These deduced values of α_1 are plotted against the corresponding e/B in Figure 4.17. The average value of α_1 from this plot is about 2.39.

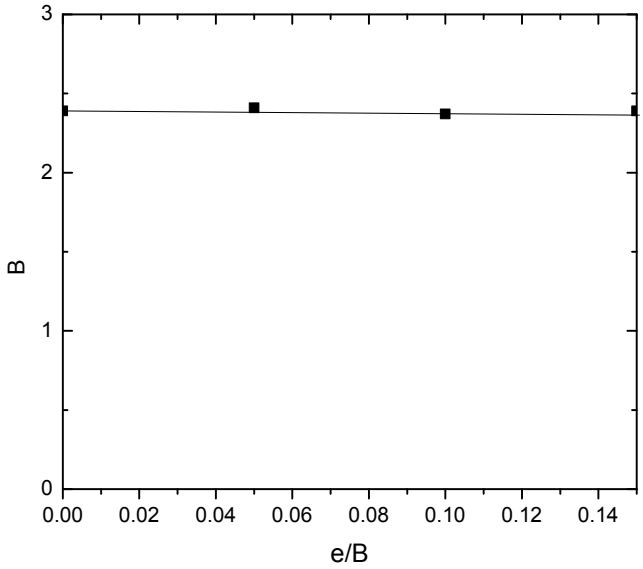

Figure 4.17: Variation of α_1 with e/B

Thus,

$$R_{KR} = 2.39\left(\frac{d_f}{B}\right)^{0.61}\left(\frac{e}{B}\right)^{0.89} \tag{4.10}$$

Table 4.3 Comparison of predicted reduction factor with those observed from experiments

Sl no	***N***	***d_f/B***	***e/B***	***$R_{KR(Expt)}$***	***$R_{KR(pred)}$***	***%Deviation***
1	2	0.6	0.05	0.125	0.12	-2.74
2		0.6	0.1	0.25	0.23	-10.88
3		0.6	0.15	0.375	0.32	-15.94
4	3	0.85	0.05	0.15	0.15	0.31
5		0.85	0.1	0.275	0.28	1.37
6		0.85	0.15	0.4	0.40	0.00
7	4	1.1	0.05	0.21	0.18	-19.26
8		1.1	0.1	0.36	0.33	-10.32
9		1.1	0.15	0.472	0.47	-0.83

4.3.3 Conclusions

The results of a number of laboratory model tests conducted to determine the ultimate bearing capacity of a square foundation supported by sand and subjected to an eccentrically load over geogrid-reinforced sand is presented here. Tests have been conducted on dense sand. All the tests were conducted in surface condition. The load eccentricity ratio e/B is varied from 0 to 0.15, and the number of geogrid layer is varied from N = 0, 2, 3 and 4. Based on the test results, following conclusions are drawn:

- A comparison of the R_{KR} values obtained from the experiments as well as predicted from experiments has been made. The same is presented in Table 4.3 it is seen that in general the deviation is within 10% except in one case it is 20%.
- It is to be pointed out that the present tests were conducted with one model footing and one type of sand. The existence of possible scale effects by changing the width of the foundation has not been verified. This may lead to changes in the magnitudes of the constants α_1, α_2 and α_3.

CHAPTER 5

NUMERICAL MODELLING

5.1 Introduction

Neural network model is developed to estimate the reduction factor (*RF*) for predicting the ultimate bearing capacity of eccentrically loaded shallow foundations on geogrid reinforced sand bed. The experimental database of Patra et al. (2006) is used for the analysis. Different sensitivity analysis was carried out to find out the important parameters affecting reduction factor. The concept of reduction factor i.e. the ratio of the ultimate bearing capacity of the foundation subjected to an eccentric load to the ultimate bearing capacity of the foundation subjected to a centric vertical load. Emphasis was given on the construction of neural interpretation diagram, based on the trained weights of the developed neural network model. An ANN model equation is developed based on the trained weights of the neural network model. Finally, the results from ANN are compared with the empirical equation given by Patra et al. (2006). The predictability of ANN equation is found to be better than empirical one.

5.2 Overview of artificial neural network

5.2.2 Biological model of a neuron

McCulloch and Pitts (1943) developed the first artificial neuron. ANNs are a form of artificial intelligence (AI), which, simulate the biological structure of the human brain and nervous system. (Shahin *et al.* 2002). The artificial neural network is related to the biological counterparts. The characteristics of brain function that inspired the development of artificial neural network. The neuron is the basic unit for processing the signals in the biological nervous system. The neurons have three principal components.

i)Dendrites, ii)cellbody. iii) axon. Each neuron receives and processes the signals from other neurons through the input paths called dendrites. The dendrites collect the signals and send them to the cell body, which sums the incoming signals. Then this charge produces an output signal.

The output signal is then transmitted to the neighboring neurons through a single long stem like fibre that is called axon. The axon of a neuron connects to dendrites of the neighboring neurons through junctions called synapses.

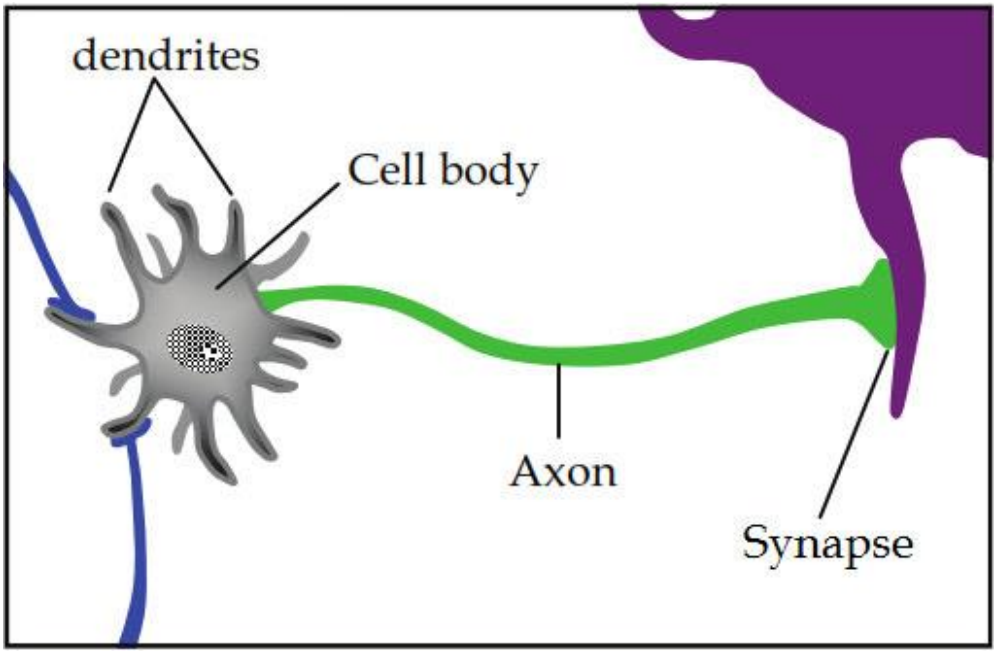

Figure 5.1: Biological neuron (after Park, 2011)

5.2.2 The concept of artificial neural network

The architecture of ANNs consists of a series of processing elements (PEs), or nodes, that are usually arranged in layers: an input, output and one or more hidden layers, as shown in Figure 5.1. The determination of number of hidden layers and the number of neurons in each hidden layer is a significant task. The number of hidden layers is usually determined first and is a critical step. The number of hidden layers required generally depends on the complexity of the relationship between the input parameters and the output value (Park, 2011).

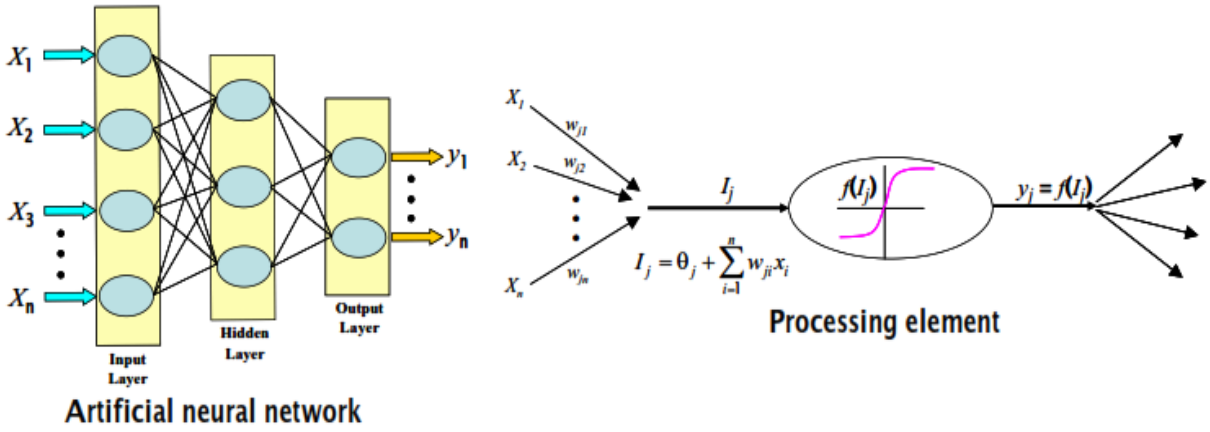

Figure 5.2: Typical structure and operation of ANN

ANNs learn from data set presented to them and use these data to adjust their weights in an attempt to capture the relationship between the model input variables and the corresponding outputs. Consequently, Artificial Neural Networks do not need prior knowledge regarding the nature of the mathematical relationship between the input and output variables. This is the most beneficial effect of ANN.

5. 2.3 Application of ANN in Geotechnical Engineering

In case of many geotechnical engineering problems ANNs have been applied and have demonstrated some degree of success such as ANNs have been used in pile bearing capacity prediction, stress-strain modeling of sands interpretation of site investigation, seismic liquefaction assessment, earth retaining structures, settlement of structures, slope stability, liquefaction, soil compaction, soil swelling and classification of soils.

5.3 Problem Definition

Develop a neural network model from the results of extensive laboratory model tests conducted by Patra et al. (2006) .Extensive laboratory model tests have been conducted on a strip footing lying over sand bed subjected to an eccentric load to determine the ultimate bearing capacity .The ultimate bearing capacity of footing at any depth of embedment subjected to eccentric load

can be determined by knowing the ultimate bearing capacity of footing subjected to centric and vertical load at that depth of embedment and the corresponding reduction factor. This reduction factor (*RF*) is the ratio of the ultimate bearing capacity of strip footing on geogrid reinforced soil subjected to an eccentric load to the ultimate bearing capacity of the footing subjected to a centric vertical load at the same depth of embedment.

In the present study, the feedforward backpropagation neural network is trained with Levenberg-Marquadrt algorithm, which is known as Levenberg-Marquadrt neural network (LMNN). Based on the trained weights of the developed neural network different sensitivity analysis are carried out to study the important parameters and Neural Interpretation Diagram (NID) is constructed to find out the direct or inverse effect of input parameters on the output. A prediction model equation is developed with the weights of the neural network as the model parameters. Furthermore, the developed reduction factor is compared with the developed empirical equation by Patra et al. (2006).

5.4 Database and Preprocessing

The laboratory experimental data used for neural network model is presented in Table 5.1. The database consist of parameters like load eccentricity (*e*), embedment ratio (d_f /*B*).Thirty six numbers of laboratory model tests results as conducted in this series have been considered for analysis. In this ANN model, two dimensionless input parameters are *e* / *B*and d_f /*B* and the output is reduction factor (*RF)*.

$$d_f = d + D_f \tag{5.1}$$

Where, *d* = depth of Reinforcement measured from the bottom of the foundation.

D_f = depth of foundation.

$$\frac{q_{UR(e/B,d_f/B)}}{q_{UR(e/B=0,d_f/B)}} = RF \tag{5.2}$$

Reduction factor (R_{KR}) based upon Patra et.al. (2006) is given as below

$$\frac{q_{UR(e/B,d_f/B)}}{q_{UR(e/B=0,d_f/B)}} = 1 - R_{KR} \tag{5.3}$$

Where, $q_{UR(e/B,d_f/B)}$, =Ultimate bearing capacity of footing with eccentricity ratio e/B at an embedment ratio of d_f/B on geogrid reinforced soil and $q_{UR(e/B=0,d_f/B)}$ =Ultimate bearing capacity of footing with centric vertical loading (e/B = 0) at the same of embedment ratio.

Out of 36 test records as shown in Table 5.1, 27 tests are considered for training and the remaining 9 are reserved for testing. Each record represents a complete model test where an eccentrically loaded strip footing supported by geogrid reinforced sand bed was subjected to failure. All the variables (i.e. inputs and output) are normalized in the range [-1, 1] before training. A feed forward back-propagation neural network is used with hyperbolic tangent sigmoid function and linear function as the transfer function. The backpropagation algorithm trains the network by iteratively adjusting all the connection weights among neurons, with the goal of finding a set of connection weights that minimizes the error of the network, i.e. sum-of-the-squares between the actual and predicted output (least squares error function, Olden 2000). A feedforward neural network has one-way connection to other units. Inputs are passed from layer to layer in a feed-forward manner. In the model, each input unit is connected to each hidden unit and then each hidden unit is connected to each output unit Ozesmi and Ozesmi 1999).The network is trained (learning) with Levenberg–Marquardt (LM) algorithm as it is efficient in comparison to gradient descent back-propagation algorithm (Goh et al. 2005; Das and Basudhar 2006). The ANN has been implemented using MATLAB V 7.11.0 (R2010b).

Table5.1. Dataset used for training and testing of ANN model

Data type **(1)**	**Expt. No.** **(2)**	$\frac{e}{B}$ **(3)**	d_f/B **(4)**	q_u(kN/m^2) **(5)**	**Experimental** RF **(6)**
Training	1	0.05	0.6	174	0.845
	2	0.1	0.6	133	0.646
	3	0.15	0.6	85.5	0.415
	4	0	0.85	254	1.000
	5	0.05	0.85	222	0.874
	6	0.1	0.85	178	0.701
	7	0	1.1	336	1.000
	8	0.05	1.1	296	0.881
	9	0.15	1.1	178	0.530
	10	0	1.35	393	1.000
	11	0.1	1.35	289	0.735
	12	0.15	1.35	223	0.567
	13	0.05	1.6	440	0.875
	14	0.1	1.6	355	0.706
	15	0.15	1.6	250	0.497
	16	0	1.85	584	1.000
	17	0.05	1.85	513	0.878
	18	0.1	1.85	423	0.724
	19	0	2.1	667	1.000

Data type **(1)**	**Expt. No.** **(2)**	$\frac{e}{B}$ **(3)**	d_f/B **(4)**	q_u(kN/m^2) **(5)**	**Experimental** ***RF*** **(6)**
	20	0.05	2.1	578	0.867
	21	0.15	2.1	355	0.532
	22	0	1.1	311	1.000
	23	0.1	1.1	228	0.733
	24	0.15	1.1	159	0.511
	25	0.05	1.6	393	0.866
	26	0.1	1.6	328	0.722
	27	0.15	1.6	240	0.529
Testing	28	0	0.6	206	1.000
	29	0.15	0.85	123	0.484
	30	0.1	1.1	239	0.711
	31	0.05	1.35	345	0.878
	32	0	1.6	503	1.000
	33	0.15	1.85	317	0.543
	34	0.1	2.1	478	0.717
	35	0.05	1.1	280	0.900
	36	0	1.6	454	1.000

5.5 Results and Discussion

The maximum, minimum, average and standard deviation values of the two inputs and one output parameters used in the ANN model are presented in Table 2. They are computed from the database. The schematic diagram of ANN architecture is shown in Figure 2. The number of hidden layer neurons is varied and the mean square error (mse) was noted found to be 0.001 when there were two neurons in the hidden layer [Figure 3]. Therefore, the final ANN architecture is retained as 2-2-1 [i.e. 2 (input) – 2 (hidden layer neuron) – 1 (Output)].Mean Square Error (MSE) is defined as

$$MSE = \frac{\sum_{i=1}^{n} \left(RF_i - RF_p \right)^2}{n} \tag{5.4}$$

Coefficient of efficiency, R^2 is expressed as

$$R^2 = \frac{E_1 - E_2}{E_1} \tag{5.5}$$

where

$$E_1 = \sum_{i=1}^{n} \left(RF_i - \overline{RF} \right)^2 \tag{5.6}$$

and

$$E_2 = \sum_{i=1}^{n} \left(RF_P - RF_i \right)^2 \tag{5.7}$$

Where $RF_i, \overline{RF}, and\ RF_p$ are the experimental, average experimental and predicted *RF* values respectively.

n = number of training data

Table5.2. Statistical values of the parameters

Parameter	**Maximum value**	**Minimum value**	**Average value**	**Standard Deviation**
e/B	0.15	0	0.075	0.056
d_f/B	2.1	0.6	1.35	0.456
RF	1	0.415	0.774	0.185

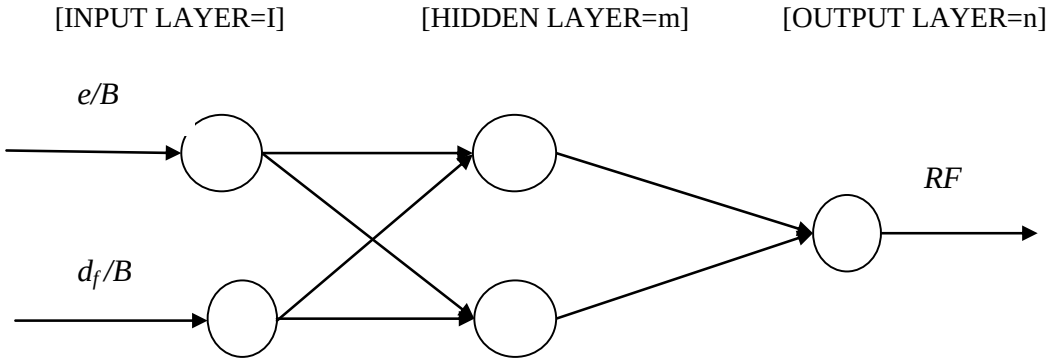

Figure .5.3: The ANN Architecture

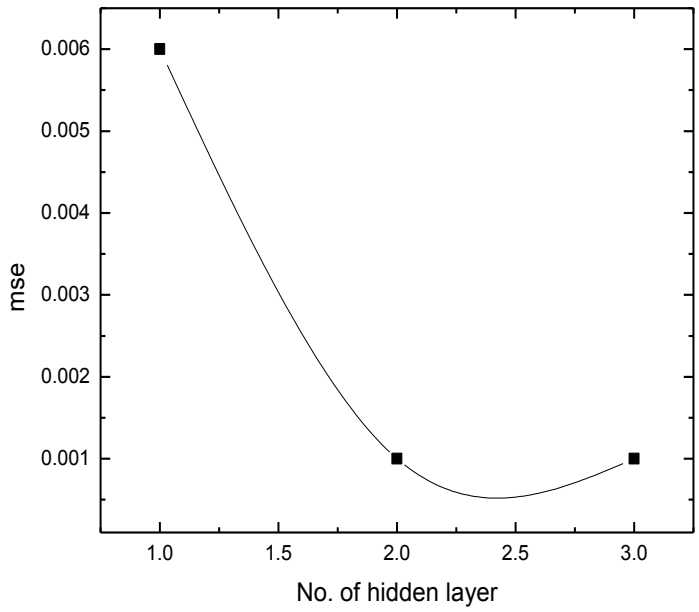

Figure.5.4: Variation of hidden layer neuron with mean square error (mse)

The coefficient of efficiency (R^2) are found to be 0.9964 for training & 0.9976 for testing as shown in Figures 5.5 and 5.6. Data used in this analysis have been obtained from laboratory model tests. The details of the model tests are given below:

The model foundation used for this study had a width of 80 mm and length of 360 mm. It was made out with a mild steel plate with thickness of 25 mm. The bottom of the model foundation was made rough by coating it with glue and then rolling it over sand. Bearing capacity tests were conducted in a box measuring 0.8m (length)*0.365m (width)*0.7m (depth).The inside walls of the box and edges of the model were polished to reduce friction as much as possible. The sides of the box are heavily braced to avoid lateral yielding. Locally available sand was used for the present model tests. The used for the tests had 100% passing 0.7 mm size sieve and 0% passing 0.3 mm size sieve. For all the tests, the average unit weight and the relative density of compaction were kept at 14,81KN/m^3 and 72% respectively. The average peak friction angle ϕ'

of the sand at the tests conditions are determined from direct shear tests was 42.4°.Tensar biaxial geogrid (BX1100) was used for the present tests. In conducting a model test, sand was placed in lift of 25 mm in the test box. For each lift, the amount of the soil required to produce the desired unit weight was weighed and compacted using a flat bottom wooden block. Geogrid layers are placed in the sand at desired values of *u/B* and *h/B* .The model foundation was placed on the surface as well as at desired depths below the surface of the sand bed. Centric or eccentric load have been applied to the model foundation by an electrically operated hydraulic jack. Two dial gauges are used and having 0.01-mm accuracy placed on either side of the model foundation recorded the settlement of the foundation.. For the present test program, the following parameters were adopted for the geogrid reinforcement layers: *u/B* =0.35, *h/B* =0.25, *b/B*=5. All the data used in the training and the testing are from the same source and are of same nature. Probably, this may be one of the causes for better fitting in both testing and training phase as well. The weights and biases of the network are presented in Table.3.These weights and biases can be utilized for interpretation of relationship between the inputs and output, sensitivity analysis and framing an ANN model in the form of an equation. The residual analysis was carried out by calculating the residuals from the experimental reduction factor and predicted reduction factor for training data set. Residual (e_r) can be defined as the difference between the experimental and predicted *RF* value and is given by

$$e_r = RF_i - RF_p \tag{5.8}$$

The residuals are plotted with the experiment number as shown in Figure 5.7. It is observed that the residuals are distributed evenly along the horizontal axis of the plot. Therefore, it can be said that the network is well trained and can be used for prediction with reasonable accuracy.

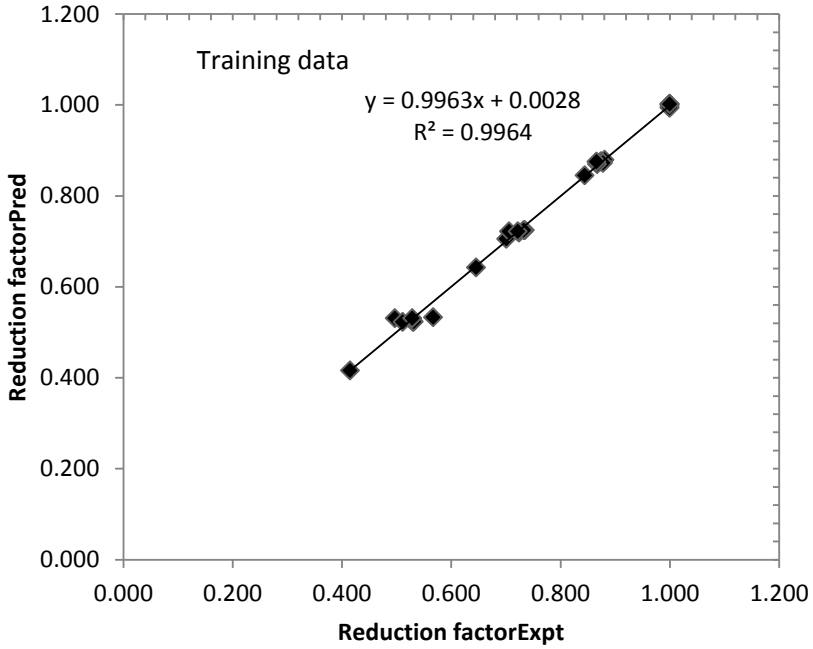

figuer.5.5: Correlation between Predicted Reduction Factor with Experimental Reduction Factor for training data

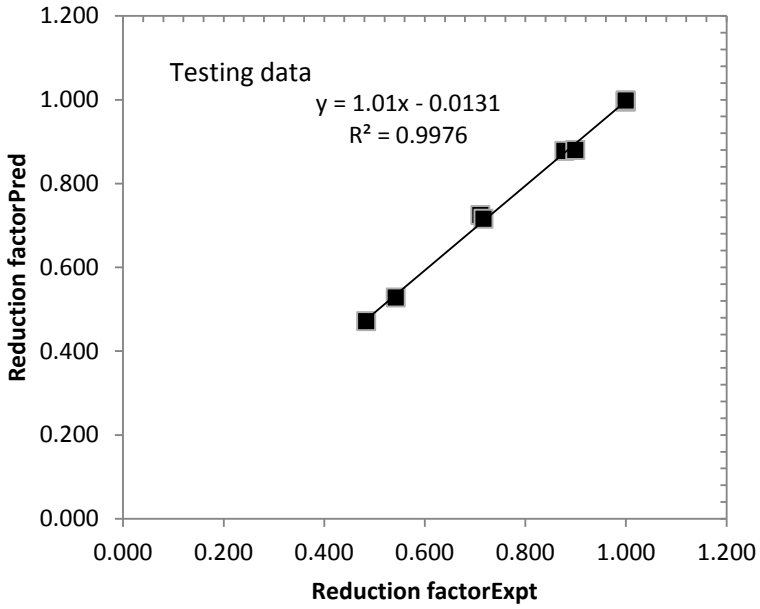

Figure .5.6: Correlation between Predicted Reduction Factor with Experimental Reduction Factor for testing data

Table5.3. Values of connection weights and biases

Neuron	Weight			Bias	
	W_{iK}		w_k		
	e/B	d_f/B	*RF*	b_{hk}	b_0
Hidden Neuron 1 (k=1)	1.1141	-3.0435	-0.2553	-3.1742	-61.3437
Hidden Neuron 2 (k=2)	-0.1711	-0.0064	63.7472	1.9935	

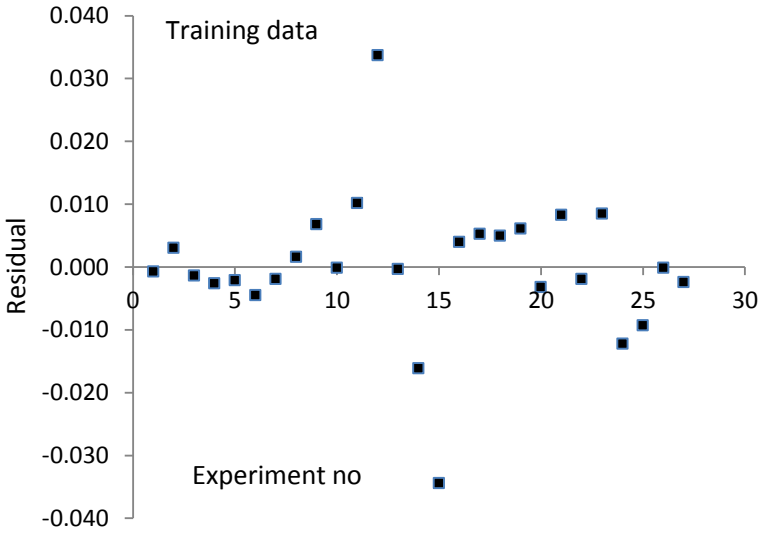

Figure 5.7: Residual distribution of training data

5.5.1 Sensitivity Analysis

Sensitivity analysis is carried out for selection of important input variables. Different approaches have been suggested to select the important input variables. The Pearson correlation coefficientis considered as one of the variable ranking criteria in selecting proper inputs for the ANN (Guyon

and Elisseeff 2003; Wilby et al. 2003). Garson (1991) proposed a method, later on modified by Goh (1995), for partitioning the neural network connection weights in order to determine the relative importance of each input variable in the network. It is important to mention that Garson's algorithm uses the absolute values of the connection weights when calculating variable contributions, and therefore does not provide the information on the effect of input variables in terms of direct or inverse relation to the output. Olden et al. (2004) proposed a connection weights approach based on the NID, in which the actual values of input-hidden and hidden-output weights are taken. It sums the products across all the hidden neurons, which is defined as S_i. The relative inputs are corresponding to absolute S_i values, where the most important input corresponds to highest S_i value. The details of connection weight approach are presented in Olden et al. (2004).

Table 5. 4. Cross-correlation of the input and output for the reduction factor

Parameters	***e/B***	***d_f/B***	***RF***
e/B	1	0	-0.986
D_f/B		1	0.06
RF			1

Table 5.4 shows the cross correlation of inputs with the reduction factor. From the table it is observed that *RF* is highly correlated to *e/B* with a cross correlation values of 0.986, followed by d_f */B*. The relative importance of the two input parameters as per Garson's algorithm is presented in Table 5.5. The *e/B* is found to be the most important input parameter with the relative importance value being 61.59% followed by 38.40% for d_f */ B*. The relative importance of the present input variables, as calculated following the connection weight approach (Olden et al.

2004) is also presented in Table 5.The*e/B* is found to be the most important input parameter (S_i value =-11.1916) followed by d_f / B (S_i value =0.369). The S_i values being negative imply that *e/B*are indirectly and d_f /B is directly related to *RF* values. In other words, increasing *e/B* will lead to a reduction in the *RF* and hence leads to lower ultimate bearing capacity. Increasing d_f / B increases the *RF*, and hence increases the bearing capacity

Table.5.5: Relative Importance of different inputs as per Garson's algorithm and Connection weight approach

Parameters	**Garson's algorithm**		**Connection weight approach**	
(1)	Relative Importance (%) (2)	Ranking of inputs as per relative importance (3)	$S_i$values as per Connection weight approach (4)	Ranking of inputs as per relative importance (5)
e /B	61.59	1	-11.191	1
D_f / B	38.40	2	0.369	2

5.5.2 Neural Interpretation Diagram (NID)

Ozesmi and Ozesmi (1999) proposed the Neural Interpretation Diagram (NID) for providing a visual interpretation of the connection weights among neurons, where the relative magnitude of each connection weight is represented by line thickness (i.e. magnitude of weights is proportional to line thickness) and line shading represents the direction of the weight (i.e. solid lines denote positive, excitatory signals and dashed lines denote negative, inhibitor signals). The relationship between the inputs and outputs is determined in two steps since there are input-

hidden layer connections and hidden-output layer connections. Positive effects of input variables are depicted by positive input-hidden and positive hidden-output connection weights, or negative input-hidden and negative hidden-output connection weights. Negative effects of input variables are depicted by positive input-hidden and negative hidden-output connection weights, or by negative input-hidden and positive hidden-output connection weights. Therefore, the multiplication of the two connection weight directions (positive or negative) indicates the effect that each input variable has on the output variable. The input directly related to the output is represented with a grey circle and that having inverse effect with blank circle.

It is seen from Table 5.5 (4^{th} Column) that S_i values for parameters (e/B) are negative indicating that the parameters (e/B) are inversely related to RF values, whereas S_i value for parameter (d_f/B) being positive is directly related to RF values. This is shown in Figure 5.8. The ANN model is not a "black box" model and could explain the physical effect of the input parameters on the output.

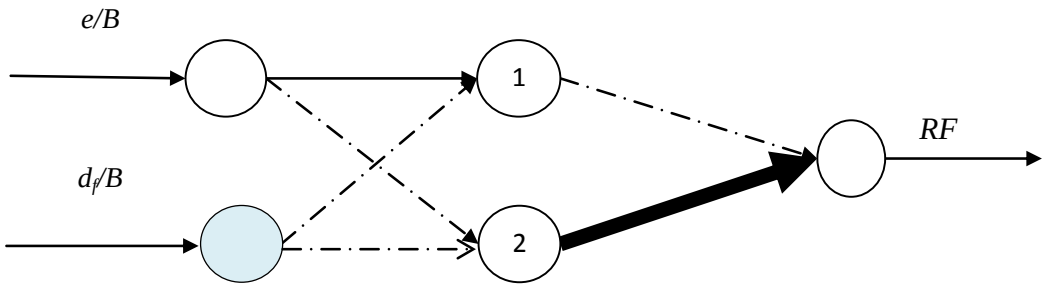

Figure 5.8: Neural Interpretation Diagram (NID) showing lines representing connection weights and effects of inputs on Reduction Factor (RF)

5.5.3 ANN model equation for the Reduction Factor based on trained neural network

A model equation is developed with the weights obtained from trained neural network as the model parameters (Goh et al. 2005). The mathematical equation relating input parameters (e/B, d_f / B) to output (Reduction Factor) can be given by

$$RF_n = f_n\left\{b_0 + \sum_{k=1}^{h}\left[w_k\, f_n\left(b_{hk} + \sum_{i=1}^{m} w_{ik} X_i\right)\right]\right\} \tag{5.9}$$

where RF_n= normalized value of RF in the range [-1, 1], f_n= transfer function, h = no. of neurons in the hidden layer, X_i= normalized value of inputs in the range [-1, 1], m = no. of input variables, w_{ik} = connection weight between i^{th} layer of input and k^{th} neuron of hidden layer, w_k = connection weight between k^{th} neuron of hidden layer and single output neuron, b_{hk} = bias at the k^{th} neuron of hidden layer, and b_o = bias at the output layer.

The model equation for Reduction Factor of eccentrically loaded strip foundation supported by geogrid reinforced sand bed was formulated using the values of the weights and biases shown in Table 3as per the following steps.

Step – 1

The input parameters were normalized in the range [-1, 1] by the following expressions

$$X_n = 2\left(\frac{X_1 - X_{\min}}{X_{\max} - X_{\min}}\right) - 1 \tag{5.10}$$

where, X_n= Normalized value of input parameter X_1, and X_{max} and X_{min} are maximum and minimum values of the input parameter X_1 in the data set.

Step – 2

Calculate the normalized value of reduction factor (RF_n) using the following expressions

$$A_1 = 1.1141(e/B)_n - 3.0435(d_f/B)_n - 3.1742 \tag{5.11}$$

$$A_2 = -0.1711(e/B)_n - 0.0064(d_f/B)_n + 1.9935 \tag{5.12}$$

$$B_1 = -0.2553\left(\frac{e^{A_1} - e^{-A_1}}{e^{A_1} + e^{-A_1}}\right) \tag{5.13}$$

$$B_2 = 63.7472\left(\frac{e^{A_2} - e^{-A_2}}{e^{A_2} + e^{-A_2}}\right) \tag{5.14}$$

$$C_1 = -61.3437 + B_1 + B_2 \tag{5.15}$$

$$RF_n = C_1 \tag{5.16}$$

Step – 3

Demoralize the RF_n value obtained from Eq. to actual RF as

$$RF = 0.5(RF_n + 1)(RF_{\max} - RF_{\min}) + RF_{\min} \tag{5.17}$$

$$RF = 0.5(RF_n + 1)(1 - 0.415) + 0.415 \tag{5.18}$$

5.6 Comparison with empirical equation by Patra et al. (2006)

Patra et al. (2006), proposed an reduction factor (R_{KR}) for eccentrically loaded strip foundation supported by geogrid-reinforced sand which is given by

$$R_{KR} = 4.97(d_f/B)^{-0.12}(e/B)^{1.21} \tag{5.19}$$

$$\frac{q_{UR(e)}}{q_{UR}} = 1 - R_{KR} \tag{5.20}$$

$q_{UR(e)}$ = Ultimate bearing capacity due to eccentric loading.

R_{KR} = Reduction factor for geogrid-reinforced sand.

*To compare wit*h the present developed equation (RF), the R_{KR} will take the form as

$$RF = 1 - R_{KR} \tag{5.21}$$

$$RF = 1 - \left(4.97\left(d_f / B\right)^{-0.12}\left(e/B\right)^{1.21}\right) \tag{5.22}$$

The results for reduction factor (*RF*) obtained from developed ANN equation (Eq. 5.18) compared with the developed empirical equation of Patra et al. (2006).The comparison of present analysis with Patra et al. (2006) is shown in Figure 5.9 and in Table 5.6 The comparison seems to be reasonably good. Hence, artificial neural network can be effectively used for the prediction of ultimate bearing capacity in geogrid reinforced soil under eccentric load.

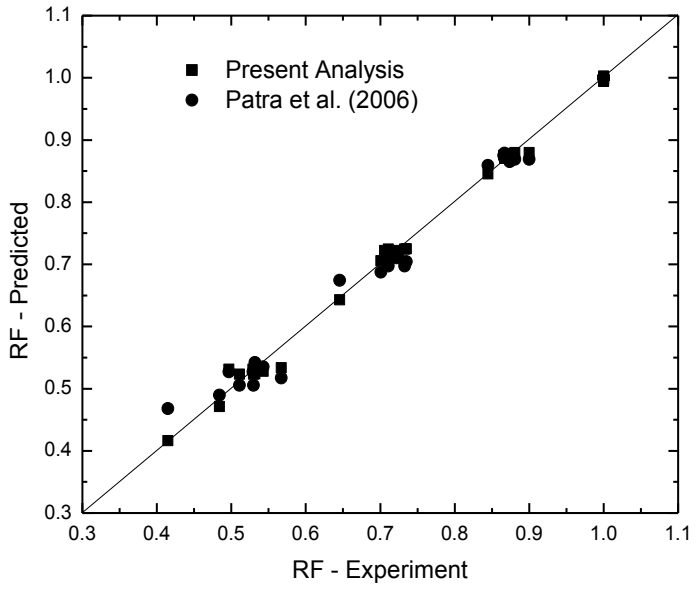

Figure 5.9: Comparison of Reduction Factor of Present analysis with Eqn in eccentric inclined load supported by geogrid-reinforced sand

Table 5.6 :Comparison of predicted reduction factor with those observed from experiments

e / B	d_f / B	q_u (kN/m^2)	RF_{expt}	RF_{ANN}	R_{KR} Patra et al. (2006)
0.05	0.6	174	0.845	0.845	0.859
0.1	0.6	133	0.646	0.643	0.674
0.15	0.6	85.5	0.415	0.416	0.468
0	0.85	254	1.000	1.003	1.000
0.05	0.85	222	0.874	0.876	0.865
0.1	0.85	178	0.701	0.706	0.688
0	1.1	336	1.000	1.002	1.000
0.05	1.1	296	0.881	0.879	0.869
0.15	1.1	178	0.530	0.523	0.505
0	1.35	393	1.000	1.000	1.000
0.1	1.35	289	0.735	0.725	0.704
0.15	1.35	223	0.567	0.533	0.517
0.05	1.6	440	0.875	0.875	0.875
0.1	1.6	355	0.706	0.722	0.710
0.15	1.6	250	0.497	0.531	0.527
0	1.85	584	1.000	0.996	1.000
0.05	1.85	513	0.878	0.873	0.877
0.1	1.85	423	0.724	0.719	0.715
0	2.1	667	1.000	0.994	1.000
0.05	2.1	578	0.867	0.870	0.879

0.15	2.1	355	0.532	0.524	0.542
0	1.1	311	1.000	1.002	1.000
0.1	1.1	228	0.733	0.725	0.697
0.15	1.1	159	0.511	0.523	0.505
0.05	1.6	393	0.866	0.875	0.875
0.1	1.6	328	0.722	0.722	0.710
0.15	1.6	240	0.529	0.531	0.527
0	0.6	206	1.000	0.995	1.000
0.15	0.85	123	0.484	0.471	0.490
0.1	1.1	239	0.711	0.725	0.697
0.05	1.35	345	0.878	0.878	0.872
0	1.6	503	1.000	0.998	1.000
0.15	1.85	317	0.543	0.528	0.535
0.1	2.1	478	0.717	0.716	0.720
0.05	1.1	280	0.900	0.879	0.869
0	1.6	454	1.000	0.998	1.000

5.7 Conclusions

Based on developed neural network model following conclusions may be drawn

- As per residual analysis, the errors are distributed evenly along the horizontal axis. It can be concluded that the network is well trained and can predict the result with reasonable accuracy.

- Based on Pearson correlation coefficient and Garson's algorithm, it was observed that *e/B* is the most important input parameter followed by d_f */B*.
- As per connection weight approach *e/B* is found to be the most important input parameter followed by d_f */B*. Hence, it may be concluded that sensitivity analysis using Connection weight approach is able to explore the inputs-output relationship using trained weights.
- The developed ANN model could explain the physical effect of inputs on the output, as depicted in NID. It was observed that *e/B* was inversely related to *RF* values whereas d_f */ B* was directly related to *RF*. Model equation is developed based on the trained weights of the ANN.

CHAPTER 6

CONCLUSIONS

AND

SCOPE FOR FUTURE

RESEARCH WORK

6.1 Conclusions

The results of laboratory model tests conducted to determine the ultimate bearing capacity of a square footing supported by multi-layered geogrid reinforced sand bed subjected to eccentric load have been reported. Tests have been conducted on dense sand. The load eccentricity ratio *e*/*B* has been varied from 0 to 0.15, and the number of geogrid layers has been varied from 2 to 4. Based on limited number of experiments conducted in laboratory an empirical equation has been developed for predicting the bearing capacity of square foundation on multi-layered geogrid reinforced sand subjected to eccentric load.

In addition to the above, an ANN model has been developed for the case of bearing capacity prediction of eccentrically loaded strip footing on geogrid-reinforced sand taking the database from Patra et al. (2006). The following are the conclusions:

- For similar reinforcement conditions, the ratio of the ultimate bearing capacity of eccentrically loaded foundations to that loaded centrally can be related by a reduction factor. The reduction factor (R_{kR}) predicted from the present experiments done in the laboratory is expressed as:

$$R_{KR} = 2.39\left(\frac{d_f}{B}\right)^{0.61}\left(\frac{e}{B}\right)^{0.89}$$

- The reduction factor is a function of d_f / B and e/B.
- At a particular settlement, the bearing capacity will be more in case of reinforced condition than unreinforced case.
- In reinforced soil, the bearing capacity also decreases with increase in eccentricity.
- An ANN model equation has been developed for reduction factor of eccentrically loaded strip footing on geogrid-reinforced sand considering the existing database

$$RF = 0.5(RF_n + 1)(1 - 0.415) + 0.415$$

- The results for strip footing from ANN model gives better result than the empirical model developed by Patra et al. (2006) for strip footing.

6.2 Scope of future work

The present thesis pertains to the study on the bearing capacity of eccentrically loaded strip footing on dry sand bed. Due to time constraint other aspects related to shallow foundations could not be studied. The future research work should address the below mentioned points:

- The present work can be extended to foundations on cohesive soil
- Large scale study to be carried out to validate the present developed equation.
- The present work can be extended to eccentrically inclined loaded reinforced soil condition
- This work can be extended by using different density of sand (i.e. dense sand, medium dense sand)

REFERNCES

REFERENCES

Adams, M.T., and Collin, J.C. (1977). “Large model spread footing load tests on geogrid-reinforced soil foundations.” *Journal of Geotechnical and Geoenvironmental Engineering*, ASCE, 123(1), pp. 66-72.

Balla, A. (1962). "Bearing capacity of foundations." *J. Soil Mech. and Found. Div.,* ASCE, 88(5), pp. 13-34.

Bolt, A. (1982). "Bearing capacity of a homogeneous subsoil under rigid footing foundation loaded with inclined and eccentric force." *In~ynieria Morska,* 3(2), pp. 108-110.

Cichy, W., Dembicki, E., Odrobinski, W., Tejchman, A., and Zadroga, B. (1978). *Bearing capacity of subsoil under shallow foundations: study and model tests.* Scientific Books of Gdansk Technical University, Civil Engineering 22, pp. 1-214.

Das, B.M., and Omar, M.T. (1994). “The effects of foundation width on model tests for the bearing capacity of sand with geogrid reinforcement.” *Geotechnical and Geological Engineering*, 12(2), pp. 133-141.

Das, et al. (2004). “Developments on the bearing capacity of shallow foundations on geogrid-reinforced soil-a review.” *Proceedings, International Conference on Geotechnical Engineering*, Sharjah, United Arab Emirates, pp. 1-.29.

Das, S.K., and Basudhar, P.K. (2006). “Undrained lateral load capacity of piles in clay using artificial neural network .” *Computers and Geotechnics*, 33, pp. 454–459.

Das, S.K., and Basudhar, P.K. (2008). ”Prediction of residual friction angle of clays using artificial neural network.” *Engineering Geology*, 100, pp. 142-145.

DeBeer, E.E. (1965). “Bearing capacity and settlement of shallow foundations on sand.” *Proceedings, Symposium on Bearing Capacity and Settlement of Foundations, Duke University*, pp. 15-33.

Garson, G.D. (1991). “Interpreting neural-network connection weights.” *Artif. Intell. Exp.*, 6**(**7), pp. 47–51.

Goh, A.T.C. (1994). “Seismic liquefaction potential assessed by neural network.” *J. Geotech. Eng.*, ASCE, 120(90), pp. 1467-1480.

Goh, et al. (2005). “Bayesian neural network analysis of undrained side resistance of drilled shafts.” *J. Geotech. and Geoenv. Eng.*, ASCE, 131(1), pp. 84-93.

Guido, et al. (1986). “Comparison of geogrid and geotextile reinforced earth Slabs.” *Canadian Geotechnical Journal*, 23(4), pp. 435–440.

Guyon, I., and Elisseeff, A. (2003). “An Introduction to variable and feature selection.” *J.Mach. Learn. Res.*, 3, pp. 1157-1182.

Hansen, J.B. (1970). “A revised and extended formula for bearing capacity.” *Bull. No. 28*, Danish Geotechnical Institute, Copenhagen

Huang, C.C., and Menq, F.Y. (1997). “Deep-Footing and Wide-Slab effects in reinforced sandy ground.” *Journal of Geotechnical and Geoenviornmental Engineering*, ASCE, 123(1), pp. 30-36.

Ingra, T.S., and Baecher, G.B. (1983). “Uncertainty in bearing capacity of sands.” *J. Geotech. Eng.*, ASCE, 109(7), pp. 899-914.

Mahiyar, H., and Patel, A. N. (2000). “Analysis of angle shaped footing under eccentric loading.” *Journal of Geotechnical and Geoenvironmental Engineering*, ASCE, 126(12), pp. 1151-1156.

Meyerhof, G.G. (1951). "The ultimate bearing capacity of foundations." *Geotechnique,* 2, 301

Meyerhof, G.G. (1953). "An Investigation for the Foundations of a Bridge on Dense Sand." *Proceedings of the 3rd International Conference on Soil Mechanics and Foundation Engineering,* 2, pp. 66-70.

Michalowski, R.L., and You, L. (1998). "Effective width rule in calculations of bearing capacity of shallow footings." *Comp. and Geotech.*, 23, pp. 237-253.

Milovic, D. M. (1965). "Comparison between the calculated and experimental values of the ultimate bearing capacity." *Proc., 6th ICSMFE, Montreal 1965,* 2, pp. 142-144.

Kumar, et al. (2007). "Analysis of square and rectangular footings subjected to eccentric-inclined load resting on reinforced sand." *Geotech and Geological Engineering,* 25, pp. 123-127.

Olden, J. D. (2000). "An artificial neural network approach for studying phytoplankton succession." *Hydrobiologia,* 436, pp. 131-143.

Olden, et al. (2004). "An accurate comparison of methods for quantifying variable importance in artificial neural networks using simulated data." *Eco. Model.,* 178(3), pp. 389-397.

Omar, et al. (1993). "Ultimate bearing capacity of shallow foundations on sand with geogrid reinforcement." *Canadian Geotechnical Journal*, 30(3), pp. 545–549.

Ozesmi, S.L., and Ozesmi, U. (1999). "An artificial neural network approach to spatial modeling with inter specific interactions." *Eco. Model.,* 116, pp. 15-31.

Patra, et al. (2005). "Bearing capacity of embedded strip foundation on geogrid-reinforced sand." *Geotextiles and Geomembranes,* 23, pp. 454-462.

Patra, et al. (2006). "Eccentrically loaded strip foundation on geogrid-reinforced sand."*Geotextiles and Geomembranes,* 24, pp. 254–259.

Prakash, S., and Saran, S. (1971). “Bearing capacity of eccentrically loaded footings.” *Journal of Soil Mechanics and Foundation*, ASCE, 97(1), pp. 95-118.

Purkayastha, R.D., and Char, R.A.N. (1977). “Sensitivity analysis for eccentrically loaded footings.” *J.Geotech.Eng. Div*., ASCE, 103(6), 647.

Saran, S. and Agarwal, R.K. (1991). “Bearing capacity of eccentrically obliquely loaded foundation.” *J. Geotech. Eng.*, ASCE, 117(11), pp.1669-1690.

Shahin, M.A., Maier, H.R., and Jaksa, M.B. (2002). “Predicting settlement of shallow foundations using neural network.” *J. Geotech. and Geoenv. Eng.*, ASCE, 128(9), pp. 785-793.

Shin, E.C., and Das, B.M. (2000). “Experimental study of bearing capacity of a strip foundation on geogrid reinforced sand.”*Geosynthetics International*, 7(1), pp. 59-71.

Shiraishi, S. (1990). "Variation in bearing capacity factors of dense sand assessed by model loading tests." *Soils and Found.*, 30(1), pp. 17-26.

Terzaghi, K. (1943). *Theoretical Soil Mechanics*, Wiley, New York.

Terzaghi, K., and Peck, R.B. (1948). *Soil mechanics in engineering practice,* 1st Edition, John Wiley & Sons, New York.

Vesic, A.S. (1973). “Analysis of ultimate loads of shallow foundations.” *J. of Soil Mech. and Found. Div.*, ASCE, 99(1), pp. 45-73.

Yetimoglu, T., Jonathan, T. H. W., Saglamer, A. (1994). “Bearing Capacity of Rectangular Footings on Reinforced Sand.” *Journal of Geotechnical Engineering*, ASCE, 120, 12.

Zadroga, B. (1975). "Bearing capacity of inclined subsoil under a foundation loaded with eccentric and inclined forces: Part 1--method review and own model tests." *Archive of Hydroengrg.*, 22 (4), pp. 333-336.

PUBLISHED PAPERS

1. Sahu, R., Behera, R.N., Patra, C.R., (2013). "Settlement prediction of centric inclined loaded strip footing on granular soil by ANN" Symposium of sustainable infrastructure (SID), pp.195-201.

2. Sahu, R., Behera, R.N., Patra, C.R., (2013). "Bearing capacity prediction of eccentrically loaded footing on reinforced sand by ANN" 5th International Geotechnical Symposium-Incheon, 22-24 May, 2013. (Accepted)